

CONTENTS

المحتويات

| | |
|---|----|
| الكلمة الافتتاحية | 1 |
| Editorial in chief message | 2 |
| Implementation of an LTE Network designed for downtown of Gharyan city using Mentum Planet based on PGM & Q9 models. Mohamed N Aldeb ¹ , Mohamed A Alkelsh | 3 |
| Thermal Load Assessment and EnergyEfficiency Enhancement in School Buildings: A Case Study of A School Building Rodwan Ahmed. Elhashmi ¹ , Bassam Ablqasim Ablqasim ,Saadedin Omran | 12 |
| Effect of Gully Erosion on the Slope Parallel to the Al-Rujban Mountain Road NW Libya. Aboalgasem Alakhdar | 28 |
| Modelling Switch-Behaviour of Own Car vs. Public Transport (PT) Modes for Shopping Trips Case Study: Tripoli - Libya Adel Eттаieb Elmloshi | 38 |
| Comparative Analysis of Soil Resistivity Measurements Using Wenner Four-Point Method: A Case Study in Sabratha, Libya S. Mousa , I. Abood , A. Essed , M. Alhawwari ⁴ , M. Almaysawi ⁵ | 51 |
| أثر إدارة سلسلة التوريد وعلاقتها بأداء الشركات الصناعية (دراسة ميدانية على إحدى الشركات المصنعة بالسوق الليبي) محمد البهلول أحمد البكاي ، نوا رلدين التومي ، اسيل عادل جالوته | 60 |

مجلة جامعة غريان للعلوم الهندسية

الكلمة الافتتاحية

بسم الله الرحمن الرحيم

بحمد الله وتوفيقه، يسعدنا أن نضع بين أيديكم العدد الأول من مجلة جامعة غريان للعلوم الهندسية، والتي تنطلق اليوم كمجلة علمية محكمة تُعنى بنشر البحوث والدراسات والمقالات الهندسية في مختلف التخصصات، من هندسة مدنية ومعمارية وميكانيكية وكهربائية، إلى هندسة النفط والحاسوب وهندسة المواد والمعادن وغيرها من فروع الهندسة الحديثة.

يأتي إصدار هذه المجلة استجابة لحاجة ملحة لوجود منبر علمي يُعزز ثقافة البحث والابتكار، ويشجع على تبادل المعرفة والخبرات بين الأكاديميين والمهنيين والطلبة داخل جامعة غريان وخارجها، ويساهم في دفع عجلة التطور التقني والبحثي في بلادنا الحبيبة.

لقد حرصنا منذ اللحظة الأولى على أن تلتزم مجلة جامعة غريان للعلوم الهندسية بأعلى معايير الجودة الأكاديمية، من حيث تحكيم الأبحاث، وتنوع المحتوى، وشفافية النشر. ونعمل جاهدين على أن تكون المجلة واجهة مشرفة للبحث العلمي بجامعة غريان، تساهم في دعم التنمية المستدامة وتقديم حلول مبتكرة للتحديات الهندسية التي تواجه الباحثين والصناع على حد سواء.

إن هذا العدد ما هو إلا بداية لطريق طموح، نأمل أن يتطور بدعمكم ومساهماتكم القيمة، سواء من خلال نشر الأبحاث، أو التفاعل مع ما يُنشر من أفكار وتجارب، أو بإبداء المقترحات والتوصيات التي من شأنها الارتقاء بالمجلة.

نتوجه بالشكر لكل من أسهم في إنجاح هذا العدد، من أسرة التحرير، والمراجعين الأكاديميين، والباحثين، وكل من آمن بهذه المبادرة العلمية.

نسأل الله أن يوفقنا لما فيه خير العلم والمجتمع، وأن تكون مجلة جامعة غريان للعلوم الهندسية إضافة نوعية في سجل المجالات العلمية المتخصصة.

والسلام عليكم ورحمة الله وبركاته

رئيس هيئة التحرير
مجلة جامعة غريان للعلوم الهندسية



Gharyan University Journal of Engineering Science (GUJES)

Website: <http://gujes.gu.edu.ly>

email: gujes@gu.edu.ly



Gharyan University Journal of Engineering Sciences-(GUJES) Editor-in-Chief's Message

With praise to Allah and His guidance, we are pleased to present to our esteemed readers of the first issue of *Gharyan University Journal of Engineering Sciences-(GUJES)*. This journal launched today as a peer-reviewed scientific publication dedicated to the dissemination of research studies, and scholarly articles across various engineering disciplines—ranging from civil, architectural, mechanical, and electrical engineering, to petroleum, computer, materials, and metallurgical engineering, and other modern engineering fields.

The publication of this journal comes in response to the urgent need for a scientific platform that promotes a culture of research and innovation, encourages the exchange of knowledge and expertise among academics, professionals, and students—both within Gharyan University and beyond— and contributes to advancing technological and research development in our country.

From its inception, the (GUJES) has been committed to the highest standards of academic quality in terms of research review, content diversity, and publishing transparency. We strive to ensure that the journal stands as a reputable scientific platform for Gharyan University, contributing to sustainable development and providing innovative engineering solutions to the challenges faced by researchers and industry professionals alike.

This inaugural issue marks only the beginning of an ambitious journey—one we hope will continue to grow with your valuable support and contributions, whether through submitting research, engaging with published ideas and experiences, or offering suggestions and recommendations that enhance the journal's progress.

In conclusion, we extend our sincere thanks and appreciation to all those who contributed to the success of this issue: the editorial board, academic reviewers, researchers, and everyone who believed in this scientific initiative.

We pray for continued success and that the *Gharyan University Journal of Engineering Sciences (GUJES)* becomes a distinctive and impactful addition to the field of specialized scientific publications.

Peace and blessings be upon you.

Editor-in-Chief

Gharyan University Journal of Engineering Sciences-(GUJES)



Implementation of an LTE Network designed for downtown of Gharyan city using Mentum Planet based on PGM & Q9 models

Mohamed N Aldeb ¹, Mohamed A Alkelsh ^{2*}

¹ Electric & Electronic Department, University of Gharyan, Gharyan, Libya, Mohammed.aldeeb.16@gu.edu.ly

² Electric & Electronic Department, University of Gharyan, Gharyan, Libya, Mohamed.Alkelsh@gu.edu.ly

*Corresponding author: Mohamed.Alkelsh@gu.edu.ly

Abstract

With the growing demand for fast and reliable telecommunications infrastructure, deploying a Long-Term Evolution (LTE) network has become a necessity to support both economic and social development. This paper presents three proposed layouts for designing an LTE network in the downtown area of Gharyan, which represents the city's central and most densely populated zone. The project was motivated by the uneven distribution of coverage across the area, where several locations experience either a complete lack of service or very weak signal reception. The aim is to support the city's digital transformation by improving access to mobile internet and data services, which in turn enhances business performance, emergency response, public service efficiency, education, remote learning, telemedicine, and remote work opportunities. To implement this plan, the design process relied on Mentum Planet software, a tool specialized in mobile network planning, using real-world terrain and signal data provided by Almadar Company. Three different network layout designs were simulated using two built-in propagation models: the Planet General Model (PGM) and the Q9 model. These simulations were conducted to assess signal strength and coverage across the study area. The analysis showed that one of the layouts provided significantly better signal quality and broader coverage compared to the others. Moreover, the Q9 model proved more reliable in predicting signal behavior in densely built urban settings. Based on these findings, a set of technical recommendations has been developed to guide the future implementation of LTE networks in similar environments, while also addressing challenges such as terrain variations, signal interference, and infrastructure limitations. In conclusion, this work contributes to enhancing telecommunications services in Gharyan and supports broader efforts toward innovation and digital inclusion across key sectors in the region.

Keywords: LTE, 4G, Q9, PGM, Mentum Planet

1. Introduction

Telecommunication technology has witnessed remarkable advancements over the past decades, evolving from the first generation (1G), which was limited to voice communication, to the fourth generation (4G), which introduced high-speed data transmission and low latency. This transformation was driven by the growing demand for modern applications that require fast and reliable connections, such as high-definition video streaming, online gaming, and augmented and virtual reality applications. In this context, 4G LTE technology has become a cornerstone of modern digital infrastructure, offering enhanced performance and greater flexibility, particularly in densely populated areas. [1]

Despite these capabilities, several technical challenges remain especially those related to coverage quality, efficient resource distribution, and signal loss that continue to affect overall network performance. The core research problem lies in the need for accurate models capable of predicting signal losses (Path Loss) in 4G networks, which is crucial for improving network



planning and operational efficiency. Relying on unsuitable or randomly selected models may lead to weak coverage, increased interference, and a significant decline in network performance. The importance of this study stems from the widespread reliance on 4G networks, particularly in regions that have not yet transitioned to fifth-generation (5G) systems. As a result, any enhancement in the design of 4G networks has a direct impact on service quality and communication reliability, especially in the face of rising demand for wireless connectivity. Furthermore, the outcomes of such studies can serve as a foundational reference when planning for future network generations.

This study primarily aims to develop an efficient and well-structured coverage plan for a 4G network within the target area, with a focus on optimizing coverage distribution and minimizing signal losses. As part of this objective, four different mathematical models will be applied to calculate path loss. The process involves substituting data into each model's equations to compare the outcomes and identify the model that results in the smallest possible cell radius ensuring efficient network design. Following this theoretical phase, the study will move to the practical simulation stage using the Mentum Planet software, where the Q9 and PGM models will be employed to simulate the network's real-world performance. The results will then be presented and discussed in detail in the Results and Discussion section, followed by the Conclusion, which summarizes the key findings and offers recommendations for improving future network planning.

2. Planning a 4G LTE Networks

The process of planning a 4G LTE networks is a vital step in achieving optimal performance and ensuring the necessary coverage, required capacity, and expected quality for end users. This planning process relies on analyzing a range of technical and operational factors, such as identifying optimal locations for base stations, analyzing technical requirements, and assessing user behavior patterns. The tool used in this study is "Mentum Planet," which is considered one of the leading tools in the field of wireless network planning. This tool provides a range of functions that assist in designing, analyzing, and optimizing 4G LTE networks. For the theoretical models for Path Loss, the signal strength decreases due to the path distance, operating frequency, weather conditions, indoor environments, reflection, diffraction, scattering, free space loss, and absorption by environmental objects. It is also affected by different environments (such as urban, suburban, and rural areas, forests, seas, etc.). Differences in the height of the transmitting and receiving antennas also result in losses. [2]. This is where theoretical models for signal attenuation come into play, as they are an essential part of the planning process for 4G LTE networks. These models describe the behavior of the signal as it is transmitted from the transmitter to the receiver [2], helping to estimate signal loss. From this, one can gain insights into permissible path loss and the maximum cell range. There are several models used to calculate path loss, this paper discusses only four models, which are:

1. Free Space Path Loss Model [3].
2. Okumura-Hata Model [4].
3. Cost 231 Hata Model [5].
4. Lee Model [5].

For comparison of Signal Loss Estimation Models, Table 1 presents the results related to Path Loss derived from the preceding headings and the distance between the transmitter and receiver, with the received power fixed at -90 dB_m . This value is considered excellent for achieving good coverage in the downtown city. Additionally, the calculations are based on the following parameters: $f = 1800 \text{ MHz}$, transmitter power = 46 dB_m , height of the base station (h_t) = 24 m , and height of the receiver (h_r) = 1.5 m . It is also taken into account that the city is urban. In the following table, P_r denotes the received power.

Table 1: Path Loss and Distance Measurements for Urban Coverage

| Models | $d = 0.75 \text{ Km}$ | $d = 1.03 \text{ Km}$ | $d = 2.89 \text{ Km}$ |
|---------------|-----------------------------|-----------------------------|------------------------------|
| Okumura-Hata | $P_r = -85.15 \text{ dB}_m$ | $P_r = -90.09 \text{ dB}_m$ | $P_r = -106.16 \text{ dB}_m$ |
| Cost 231-Hata | $P_r = -90.10 \text{ dB}_m$ | $P_r = -95.04 \text{ dB}_m$ | $P_r = -111.11 \text{ dB}_m$ |
| Lee | $P_r = -68.46 \text{ dB}_m$ | $P_r = -73.53 \text{ dB}_m$ | $P_r = -90.02 \text{ dB}_m$ |

It is noted that the COST 231-Hata model predicts the highest loss among the models mentioned earlier, followed by the Okumura-Hata model and then the Lee model. Therefore, in this paper, the COST 231-Hata model will be taken into account to ensure the best possible coverage.

3. Simulation and Calculations

Simulation is a vital tool in network planning, allowing engineers to understand network behavior under various conditions and assess potential performance. The simulation process using Mentum Planet, a powerful tool in the field of wireless network planning, as shown in figure 1, which shows the main interface of Mentum Planet presenting the map of downtown of Gharyan city.

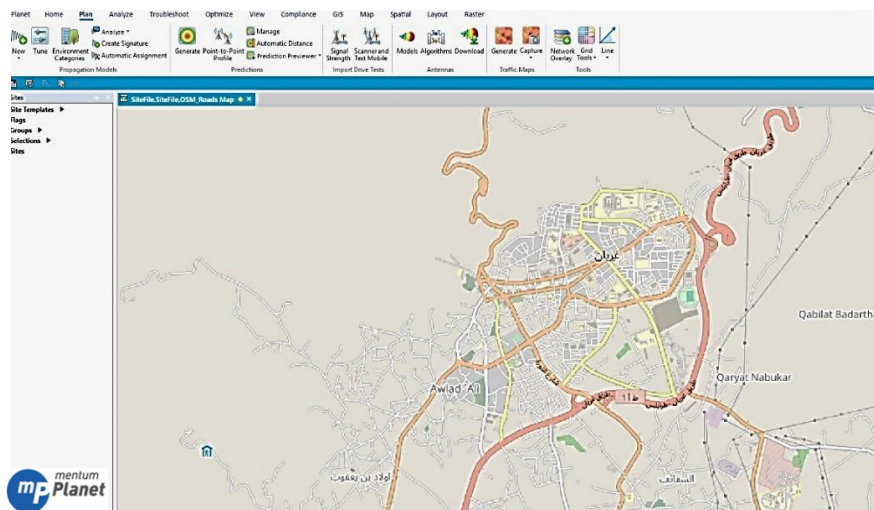


Figure 1: Main Interface of Mentum Planet showing map of downtown of Gharyan city

- **Study Site Survey:**

The downtown area is located in the middle of Gharyan city, characterized by high population density, especially during peak hours around noon. While its area is approximately 6.13 Km^2 . By implementing three different scenarios of a 4G network for the central area downtown of the city and comparing the results derived from them. Figure 2 (a) shows the downtown map as captured from Google Earth, While the Figure 2 (b) illustrates the elevation of the study area using Global Mapper.

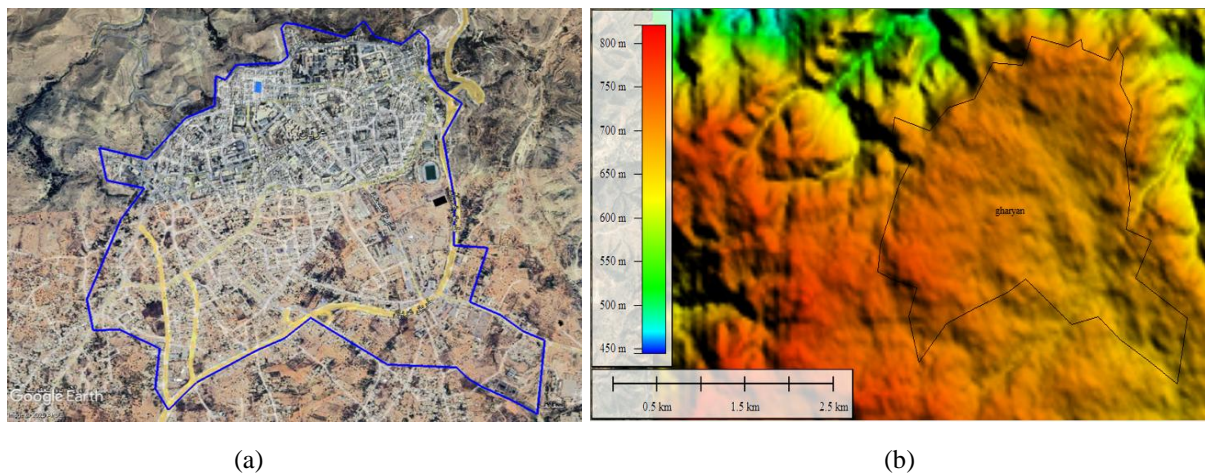


Figure 2: (a) Map of city downtown via Google Earth, (b) Digital Elevation Grid Format in Global Mapper

By assuming the radius (R) of the antenna, based on the results of the Cost 231-Hata model, which is 0.75 Km , the number of antennas needed can be calculated easily by calculating the area covered by an antenna with 3 scatterers, using the following formula: [6]

$$A = \frac{9 \cdot \sqrt{3}}{8} * R^2 \quad (1)$$

In this case:

$$A = \frac{9 * \sqrt{3}}{8} * (0.75)^2 = 1.096 \text{ Km}^2$$

From this, and from the approximate area of downtown (6.13 Km^2). It is possible to determine how many antennas are needed to cover the area, as shown:

$$\text{No. of attenas} = \frac{6.13}{1.096} = 5.593 \approx 6 \quad (2)$$

From the comparison between the previous used models, Cost 231 Hata model was found to be the most accurate in predicting path loss. For enhancing the network efficiency, its results were taken into account by using the distance it predicted when the received power was -90 dBm . However, Simulations will not be conducted using this model; instead, other existing models from Mentum Planet, which are more complex, realistic, and continuously evolving, will be used. These models include:

- **Planet General Model (PGM):**

The Planet General Model is a vital tool for cellular network planning, operating within a frequency range of 150 to 2000 MHz. It is effective for distances from 1 to 100 km, with base station antenna heights ranging from 30 to 1000 meters and mobile station antenna heights between 1 and 10 meters. This model contributes to estimating signal propagation, ensuring adequate coverage, and optimizing antenna locations based on terrain profiles, making it an ideal choice for cellular network design and given as [7]:

$$P_{RX} = P_{TX} + K_1 + K_2 \log(d) + K_3 \log(H_{eff}) + K_4 \text{Diffraction} + K_5 \log(H_{eff}) \log(d) + K_6(H_{meff}) + K_{CLUTTER} \quad (3)$$

Where:

P_{RX} is the receive power in dBm.

P_{TX} is the transmit power (ERP) in dBm.

K_1 is the constant offset in dB.

K_2 is the multiplying factor for $\log(d)$.

K_3 is the multiplying factor for $\log(H_{eff})$. It compensates for gain due to antenna height.

K_4 is the multiplying factor for diffraction calculation.

K_5 is the Okumura-Hata type of multiplying factor for $\log(H_{eff}) \log(d)$.

K_6 is the correction factor for the mobile effective antenna height gain ($K_6 H_{meff}$).

d is the distance, in meters, of the receiver from the base site.

H_{eff} is the effective height of the base site antenna from the ground.

Diffraction is the value calculated for loss due to diffraction over an obstructed path.

The value produced is a negative number, so a positive multiplication factor, K_4 is required.

$K_{CLUTTER}$ is the gain in dB for the clutter type at the mobile position in Planet DMS. In Mentum Planet, $K_{CLUTTER}$ represents a loss.

H_{meff} is the mobile effective antenna height.

- **Q9 Model:**

The Q9 model is used to estimate expected path loss between the transmitter and receiver based on terrain profiles. This model is based on the Okumura-Hata model and is particularly effective for frequencies ranging from 150 to 2000 MHz and distances from 0.2 to 100 km and given as [8]:

$$L_b = HOA + mk[\text{mobile}] + \sqrt{(a * KDFR)^2 + (JDFR)^2} \quad (4)$$

$$HOA = A_0 + A_{11} + A_2 \log(HEBK) + A_3 \log(d) \log(HEBK) - (3.2 [\log(11.75hm)]^2 + g(F)) \quad (4)$$

$$A_{11} = A_1 * \log d \quad (5)$$

$$g(F) = 44.49 \log F - 4.78(\log F)^2 \quad (6)$$

Where:

L_b is the pathloss.

$mk[\text{mobile}]$ is the land use code at the mobile in dB.

a is a parameter related to the knife-edge diffraction.

KDFR is the contribution from knife-edge diffraction in *dB*.
JDFR is the diffraction loss due to the spherical earth in *dB*.
HOA (Hata Open Area) is a variant of Okumura-Hata's equation in *dB*.
HEBK is the effective antenna height in meters as defined in the Q9 propagation model.
d is the distance from the base antenna to the mobile in *Km*.
A₀, A₁, A₂, A₃ are Q9 model tuning parameters.

Two scenarios are taken in consideration, each using one model (PGM or Q9 model). Additionally, there will be three layouts with the same antenna height, bandwidth, and receiver height, while differing in the location, number, and angles of the sectors. Table 2 presents the input data used.

Table 2: Input data

| Frequency | Base station height | Receiver height |
|-----------|---------------------|-----------------|
| 1800 MHz | 24 m | 1.5 m |

Layout 1: In this layout, six antennas were utilized and distributed to cover the entire study area, as shown in Figure 3 (a). The angles of each sector were adjusted to avoid interference, as detailed in Table 3.

Layout 2: This layout focused on the upper part of the area, which has the highest population density and a greater number of buildings, using six antennas as illustrated in Figure 3 (b). The angles of each sector were also adjusted as indicated in Table 3.

Layout 3: The number of antennas was increased to a total of nine to strengthen coverage not only in the upper area but across the entire study area, as shown in Figure 3 (c). This layout can be utilized in the future when obstacles increase and capacity needs to be expanded. The angles of each sector were adjusted as shown in Table 3.

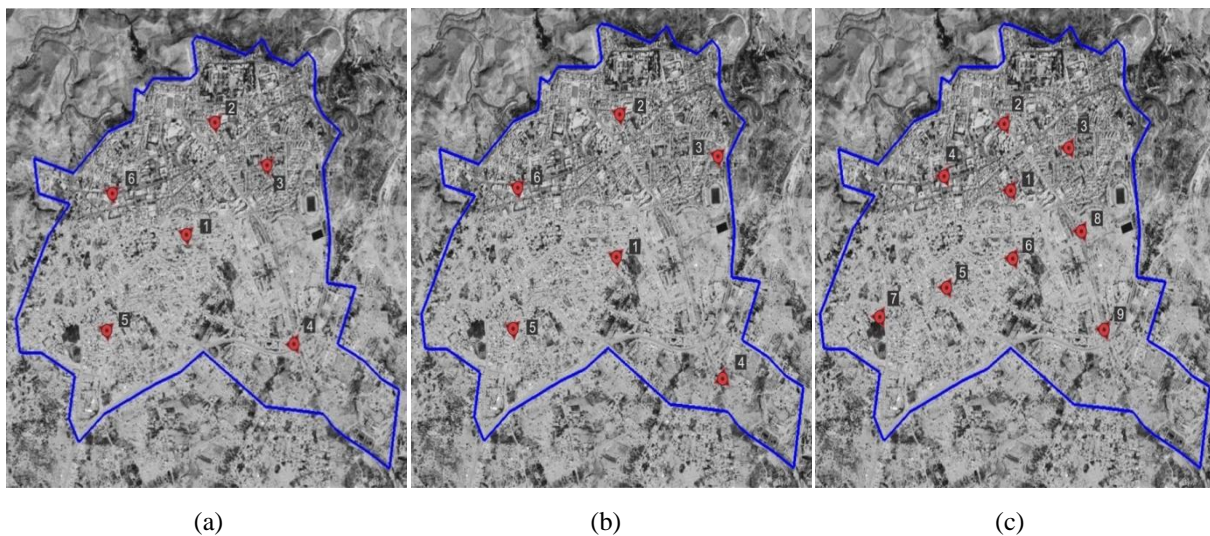


Figure 3: Antenna Distribution of (a) Layout 1 (b) Layout 2 (c) Layout 3

The following table shows the angles of each sector adjusted to avoid interference for all three layouts.

Table 3: Sector Angles for each of Layout 1, Layout 2 & Layout 3

| No. of antennas | Layout 1 | | | Layout 2 | | | Layout 3 | | |
|-----------------|----------|-----|-----|----------|-----|-----|----------|-----|-----|
| | Azimuth | | | Azimuth | | | Azimuth | | |
| 1 | 50 | 170 | 290 | 50 | 170 | 290 | 50 | 170 | 290 |
| 2 | 50 | 170 | 290 | 50 | 170 | 290 | 50 | 170 | 290 |
| 3 | 50 | 170 | 290 | 50 | 170 | 290 | 50 | 170 | 290 |
| 4 | 10 | 120 | 285 | 40 | 140 | 290 | 50 | 170 | 290 |
| 5 | 50 | 170 | 290 | 50 | 170 | 290 | 50 | 170 | 290 |
| 6 | 50 | 170 | 290 | 50 | 170 | 290 | 50 | 170 | 290 |
| 7 | | | | | | | 50 | 170 | 290 |
| 8 | | | | | | | 50 | 170 | 290 |
| 9 | | | | | | | 50 | 170 | 290 |

4. Results and Discussion

PGM Scenario: In this scenario, simulations were conducted using PGM for all layouts, and the results of each layout were presented in an image that illustrates the signal strength across the area with color codes as shown in figure 4. Additionally, there is an accompanying image that features a table displaying the received power percentage for each range throughout the entire area.

Q9 Scenario: this scenario, simulations were conducted using the Q9 model for all layouts, and the results of each layout were presented in an image that uses color coding to illustrate the signal strength across the area as shown in figure 5. Additionally, there is a subsequent image that features a table detailing the received power percentage for each range throughout the entire area.

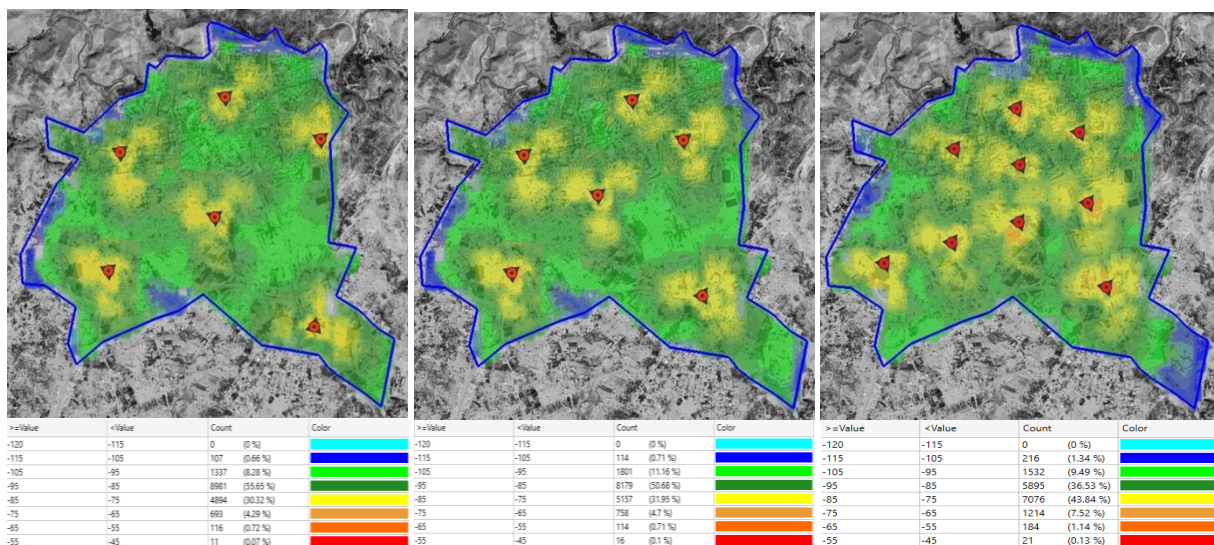


Figure 4: Coverage by Signal Level According to PGM model for (a) Layout 1 (b) Layout 2 (c) Layout 3

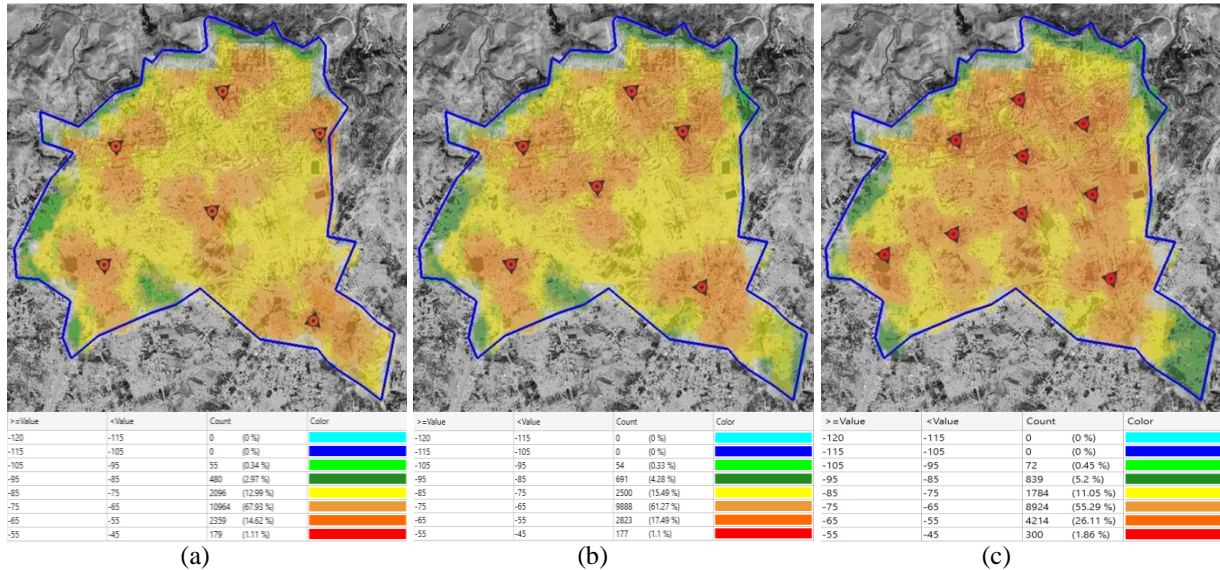


Figure 5: Coverage by Signal Level According to Q9 model for (a) Layout 1 (b) Layout 2 (c) Layout 3

Overall, the PGM was the most accurate in predicting losses. There were differences between the results of the first and second layouts, despite using the same number of antennas and having very similar antenna locations. The following tables illustrates the percentage of received power between -95 dB_m and -115 dB_m for each layout (The values were taken based on the previous mention that the minimum acceptable value for the received power is -90 dB_m . Therefore, a comparison was made between the smaller values)

Table 4: Comparison Between Layouts in Terms of Signal Level According to both models

| | Planet General Model | | Q9 Model | |
|-----------------|--|---|--|---|
| | -95 dB_m & -105 dB_m | -105 dB_m & -115 dB_m | -95 dB_m & -105 dB_m | -105 dB_m & -115 dB_m |
| Layout 1 | 8.28 % | 0.66 % | 0.34 % | 0 % |
| Layout 2 | 11.16 % | 0.71 % | 0.33 % | 0 % |
| Layout 3 | 9.49 % | 1.34 % | 0.45 % | 1 % |

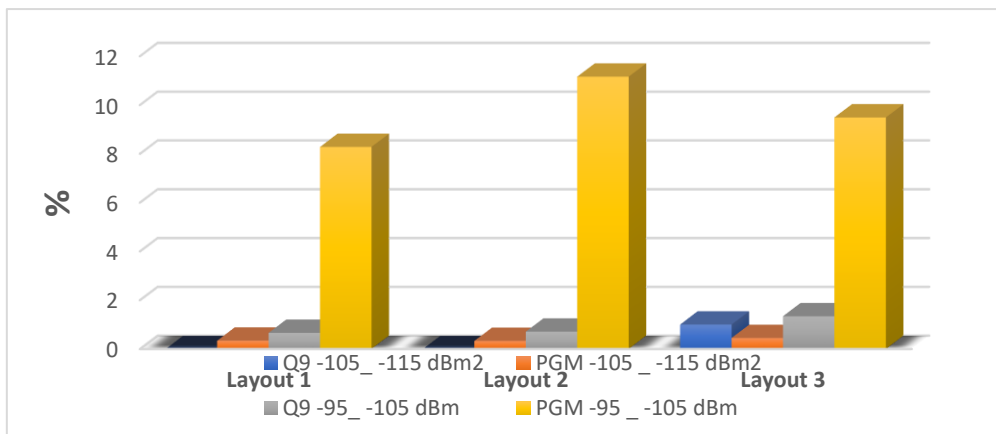


Figure 6: Error Rate Comparison Across Layouts and Signal Conditions for PGM and Q9 Models



The results predicted by the Q9 model were also quite good for all layouts, where the percentage of received power above -95 dB_m was very low. The best design is layout 1 in terms of the PGM, which is slightly better than layout 2 and also less costly than layout 3, which used more antennas than necessary. As shown in figure 6, the comparison was made based on the percentage of received power between -95 dB_m and -115 dB_m , where values below -95 dB_m are considered very good. There is a significant difference between the Cost 231 Hata model and the results from the models used by Mentum Planet, with the Q9 model being the closest to the Cost 231-Hata model.

In conclusion, one might wonder why the capacity was considered as well. The answer to this question is that the goal of this paper is to provide good receiver power throughout the study area downtown of Gharyan city. Additionally, the OFDMA technology is capable of providing substantial capacity, this means that it can be relied upon in terms of capacity.

5. Conclusion

The objective of this paper has been achieved, as it was able to provide a comprehensive plan for the downtown area of Gharyan city to ensure excellent coverage with the least number of antennas. By concluded that the location, height, and number of antennas, as well as the direction of each sector, all affect coverage and the level of loss in received power. It is also shown that the increasing of number of antennas is not always the solution. When three antennas were added, representing a significant increase, the total became nine antennas; however, the results were not as expected. The received power levels did not improve significantly within the optimal range of -45 dB_m to -65 dB_m . This emphasizes that good planning and thorough study of the area to identify the best possible locations for antennas is crucial, and it can save a lot of money by minimizing the number of antennas used.

One of these planning models could serve as a foundation upon which a company may build and improve to ultimately achieve the optimal network design.

References

- [1] E. Dahlman, S. Parkvall, & J. Skold, "4G: LTE/LTE-Advanced for Mobile Broadband", (2016).
- [2] N. Shabbir, M.T. Sadiq, H. Kashif, & R. Ullah, "Comparison of Radio Propagation Models for Long Term Evolution (LTE) Network", (2011).
- [3] M. Rani, & M. Sonia, "Design & Analysis of Propagation Models for WiMAX Communication System at 3.9 GHz", (2014).
- [4] A.E. Ibhaze, A.L. Imoize, S. O. Ajose, S. N. John, C. U. Ndujiuba, & F.E.Idachaba, "An Empirical Propagation Model for Path Loss Prediction at 2100MHz in a Dense Urban Environment", (2017).
- [5] M. Hamid, & I. Kostanic, "Path Loss Models for LTE and LTE-A Relay Stations", (2013).
- [6] T. Perets, "Dimensioning and Coverage of Molyko City by LTE Network using Atoll 3.3", (2020).
- [7] Mentum S.A, "Planet General Model Technical Note for Mentum Planet version 5.4", (2010).
- [8] Mentum S.A, "Mentum Planet User Guide for version 4.5.1", (2009).



Thermal Load Assessment and Energy Efficiency Enhancement in School Buildings: A Case Study of A School Building

Rodwan Ahmed Sh. Elhashmi^{1*}, Bassam Ablqasim Ablqasim², Saadedin Omran Elwarshfani³, Eihab Alfeetouri Altahir⁴

¹ Faculty of Engineering, Mechanical and Industrial Engineering, Gharyan University, Gharyan, Libya

² Faculty of Engineering, Mechanical and Industrial Engineering, Gharyan University, Gharyan, Libya

³ Faculty of Engineering, Mechanical and Industrial Engineering, Gharyan University, Gharyan, Libya

⁴ Faculty of Engineering, Mechanical and Industrial Engineering, Gharyan University, Gharyan, Libya

*Corresponding author: rodwan.elhashmi@gu.edu.ly

Abstract

A comprehensive study presents a detailed thermal load assessment and energy efficiency analysis of school buildings in Gharyan, Libya, with a focus on sustainable energy solutions and climate-responsive design strategies. The research addresses the critical gap in energy-efficient building practices in Libya's educational sector, where 95% of public schools rely exclusively on natural ventilation systems. Through rigorous thermal modeling and performance analysis of a representative two-story school building (910 m²), this study quantifies heating and cooling loads while evaluating the potential impact of cost-effective energy efficiency measures. The methodology employs established ASHRAE standards and thermal analysis techniques to assess building performance under Libya's hot-arid climate conditions. Key findings reveal that infiltration accounts for the highest thermal loads, while lighting and equipment contribute minimally to overall energy consumption. Implementation of comprehensive energy efficiency measures—including wall and roof insulation upgrades and high-performance window replacements—demonstrates a significant 25% reduction in total building thermal loads. This research contributes to the growing body of knowledge on energy efficiency in educational buildings within developing countries, particularly in North African contexts. The study's findings support Libya's renewable energy targets of achieving 4GW capacity by 2035, representing 20% of the national energy portfolio. The proposed energy efficiency framework provides actionable insights for policymakers, architects, and educational administrators seeking to optimize building performance while reducing operational costs and environmental impact.

Keywords: Thermal Load, Energy Efficiency, School Building, ASHRAE standards

1. Introduction

The building sector represents one of the most significant contributors to global energy consumption and greenhouse gas emissions, accounting for approximately 40% of worldwide energy use and 36% of energy-related CO₂ emissions [1]. This challenge is particularly acute in developing countries, where rapid urbanization and population growth drive increasing demand for educational infrastructure. Libya, with its population of seven million and substantial oil reserves, faces unique energy challenges that necessitate a comprehensive approach to building energy efficiency.

Libya's energy landscape has been profoundly affected by political instability and conflict since 2011, resulting in chronic electricity shortages that reached 32.5% in 2023 [2]. Despite possessing Africa's largest proven oil reserves, the country's electricity grid struggles to meet

growing demand, with most power plants relying on natural gas (67%) and oil (33%) for generation [3]. This energy crisis has been exacerbated by port blockades and civil strife, leading to massive power outages that severely impact educational institutions and other critical infrastructure.

The educational sector in Libya faces particular challenges regarding energy efficiency and indoor environmental quality. Most public secondary schools in the country are obsolete in energy terms, with 95% relying exclusively on natural ventilation to maintain classroom comfort and ensure adequate indoor air quality [4]. This reliance on passive cooling strategies, while culturally appropriate, often fails to provide optimal learning environments during extreme weather conditions, potentially impacting student health, comfort, and academic performance.

2. General Overview

2.1 Libya's Renewable Energy Potential and Policy Framework

Libya possesses exceptional renewable energy potential, particularly in solar and wind resources. The country receives solar radiation reaching 2,300 kWh/m²/year with sunshine duration of 3,500 hours annually [5]. Despite this abundant natural resource, renewable energy sources represent only 3% of the total energy supply according to the International Renewable Energy Agency (IRENA) [6]. This significant underutilization of clean energy resources presents both a challenge and an opportunity for sustainable development.

Recent policy developments indicate a growing commitment to renewable energy diversification. The Renewable Energy Authority of Libya has established ambitious targets, including achieving 10% renewable energy in the national power mix by 2025 and generating 4GW of renewable capacity by 2035, representing 20% of the total energy portfolio [7]. Major projects, such as the 500MW Sadada solar project in partnership with TotalEnergies, are currently in final development stages, with construction expected to begin in 2025 [8]. Figure 1 represents Libyan current energy mix (2024) and 2035 Libyan target energy mix.

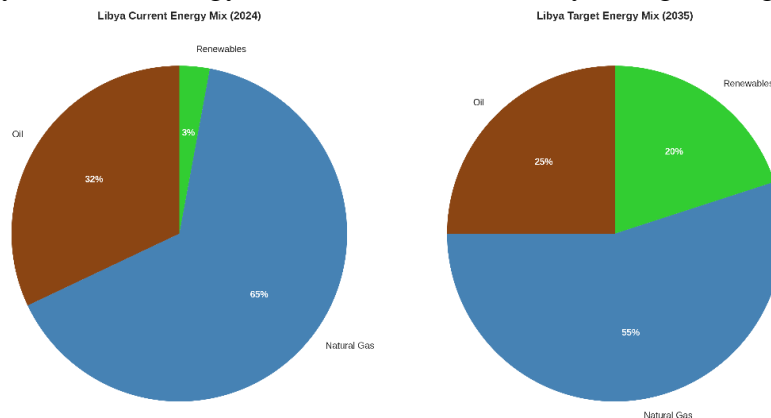


Figure 1: Libyan current and target energy mix



2.2 Energy Efficiency in Educational Buildings: Global Perspectives

The importance of energy efficiency in educational buildings extends beyond mere cost savings to encompass student health, learning outcomes, and environmental sustainability. Research by Kajjoba et al. (2025) emphasizes that buildings failing to meet thermal comfort requirements tend to consume significantly more energy for heating and cooling applications, further exacerbating energy poverty in tropical and arid regions [9]. This relationship between thermal comfort and energy consumption is particularly relevant in Libya's hot-arid climate, where cooling demands dominate energy use patterns.

International studies have demonstrated the substantial potential for energy savings in educational facilities through comprehensive efficiency measures. The American Society of Heating, Refrigerating and Air-Conditioning Engineers (ASHRAE) reports that energy-efficient design, construction, and operation can dramatically reduce building net energy use and associated greenhouse gas emissions [10]. ASHRAE consensus standards and design guides provide the technical foundation for international building practices and energy codes, making them particularly relevant for developing countries seeking to establish robust energy efficiency frameworks.

Recent research on Mediterranean schools by Llanos-Jiménez et al. (2025) reveals that thermal loads for classroom occupation typically range around 135 kJ/h·person, while lighting loads average 36 kJ/h·m² according to European standards [11]. These benchmarks provide valuable reference points for assessing the performance of educational buildings in similar climatic conditions.

2.3 Climate Change Implications and Adaptive Strategies

Climate change projections for North Africa indicate significant shifts in temperature and precipitation patterns that will further challenge building energy performance. The Intergovernmental Panel on Climate Change (IPCC) projects that much of Libya's current Mediterranean climate zones will transition to arid and semi-arid classifications by 2071-2100 under worst-case scenarios [12]. These climatic shifts will intensify cooling demands and extend overheating periods beyond traditional summer months, making energy efficiency measures increasingly critical for maintaining comfortable learning environments.

The integration of passive design strategies and renewable energy technologies emerges as a crucial adaptation mechanism for educational buildings in changing climatic conditions. Smart building platforms and renewable energy integration represent game-changing technologies that optimize energy use while enhancing grid resilience and promoting sustainability [13]. These technological solutions are particularly relevant for Libya's educational sector, where infrastructure investments must balance immediate needs with long-term climate resilience.

Despite growing recognition of energy efficiency importance in educational buildings, significant gaps remain in understanding optimal strategies for hot-arid climates, particularly in developing countries with limited resources and infrastructure constraints. Existing research



predominantly focuses on high-income regions with access to advanced technologies, leaving a critical knowledge gap regarding cost-effective solutions for countries like Libya.

This study addresses several key research gaps: (1) the lack of comprehensive thermal load assessments for educational buildings in Libya's specific climatic context, (2) limited understanding of energy efficiency potential in naturally ventilated school buildings, and (3) insufficient integration of renewable energy considerations in educational facility planning. By focusing on Gharyan, a representative city in Libya's northwestern region, this research provides insights applicable to similar educational facilities throughout the country and broader North African region.

This study makes several significant contributions to the field of building energy efficiency in developing countries. First, it provides detailed thermal modeling data for educational buildings in Libya's hot-arid climate, filling a critical gap in regional building performance literature. Second, it demonstrates the practical application of international standards (ASHRAE) in local contexts, providing a framework for future energy efficiency initiatives. Third, it quantifies the potential energy savings from specific efficiency measures, supporting evidence-based decision-making for educational infrastructure investments.

3. Methodology

3.1 Research Framework and Approach

This study employs a comprehensive building energy assessment methodology that integrates thermal modeling, performance analysis, and energy efficiency evaluation techniques. The research framework follows established international standards, primarily ASHRAE guidelines, while adapting methodologies to Libya's specific climatic and infrastructural context. The methodology is organized into four primary phases: (1) building characterization and data collection, (2) thermal load calculation and modeling, (3) energy efficiency measure implementation, and (4) performance impact assessment.

The research adopts a case study approach, focusing on a representative two-story school building in Gharyan, Libya (32.1718° N, 13.0184° E). This location was selected due to its representative climatic conditions for Libya's northwestern region and its typical educational building characteristics. The building serves as an archetype for similar educational facilities throughout the country, enabling broader applicability of research findings.

3.2 Case Study Building Characteristics

The selected school building represents a typical educational facility in Libya's public education system. The structure comprises a two-story building with a total floor area of 910 m², excluding the theater space which is utilized only during special events. The building layout includes 10 classrooms, 120 m² of office space, 4 laboratory facilities, and one theater with 120 m² floor area. The theater area was excluded from thermal load calculations due to its

intermittent occupancy pattern and the assumption that during special events, no heating or cooling is required for the remainder of the building.

The building's architectural characteristics reflect typical construction practices in Libya's educational sector. Wall construction consists of concrete block with cement plaster finishes, while the roof structure employs reinforced concrete with minimal insulation. Windows are predominantly single-pane glass with aluminum frames, representing standard specifications for public educational buildings constructed in the past several decades.

Table 1: Building Characteristics Summary

| Parameter | Specification | Value |
|-----------------------|-----------------------|--------------------|
| Total Floor Area | Excluding theater | 910 m ² |
| Number of Classrooms | Standard size | 10 units |
| Office Space | Administrative areas | 120 m ² |
| Laboratory Facilities | Science/computer labs | 4 units |
| Occupancy Capacity | Students and staff | ~300 persons |
| Construction Type | Concrete block/RC | Standard |
| Window Type | Single-pane aluminum | Standard |

3.3 Thermal Load

The thermal load calculation methodology follows established ASHRAE procedures while incorporating specific adaptations for Libya's climatic conditions and building practices. The analysis considers all major heat transfer mechanisms affecting building energy performance, including conduction through building envelope components, solar heat gain through windows, internal heat generation from occupants and equipment, and infiltration/ventilation loads.

3.4 Conductive Heat Transfer Analysis

Heat transfer through building envelope components (walls, roof, windows, and floor) was calculated using steady-state thermal resistance methods. For multi-layer building components, total thermal resistance equals the sum of individual layer resistances plus convective resistances at interior and exterior surfaces.

The general equation for heat transfer through building envelope components is:

$$Q = U \cdot A \cdot \Delta T \quad (1)$$

Where:

Q = heat transfer rate (W),

U = overall heat transfer coefficient (W/m²·°C),

A = surface area (m²), ΔT = temperature difference (°C).

Overall heat transfer coefficients were determined by inverting total thermal resistance:

$$U = \frac{1}{R_{tot}} \quad (2)$$

Where

R_{total} includes material resistances and surface convection resistances. ASHRAE recommended values for exterior surface heat transfer coefficient ($h_o = 34.0 \text{ W/m}^2 \cdot ^\circ\text{C}$) and interior surface coefficients ($h_i = 8.29 \text{ W/m}^2 \cdot ^\circ\text{C}$ for walls, $9.26 \text{ W/m}^2 \cdot ^\circ\text{C}$ for ceilings) were applied throughout the analysis.

3.5 Solar Heat Gain Calculations

Solar heat gain through windows represents a critical component of cooling loads in Libya's high-radiation environment. The methodology employs solar heat gain coefficient (SHGC) values to determine transmitted solar energy:

$$Q_{solar} = SHGC \times A_{window} \times I_{solar} \quad (3)$$

Where:

Q_{solar} = solar heat gain (W)

SHGC = solar heat gain coefficient (dimensionless)

A_{window} = window area (m^2), I_{solar} = incident solar radiation (W/m^2).

Solar heat gain coefficients were selected based on window specifications, with single-pane clear glass typically exhibiting SHGC values around 0.8. The analysis accounts for seasonal and diurnal variations in solar radiation intensity and angle of incidence.

3.6 Internal Heat Generation

Internal heat gains from occupants, lighting, and equipment were calculated based on ASHRAE standards adapted for educational building use patterns. Occupant heat generation varies with activity level and age, with children generating approximately 75% of adult heat production rates according to ASHRAE Fundamentals.

Table 2: Internal Heat Generation Rates

| Source | Sensible Heat | Latent Heat | Total Heat |
|----------------|---------------------|-------------|---------------------|
| Adult (seated) | 70 W | 45 W | 115 W |
| Child (seated) | 53 W | 34 W | 87 W |
| Lighting | 15 W/m ² | 0 W | 15 W/m ² |

3.7 Infiltration and Ventilation Loads

Infiltration represents uncontrolled air leakage into and out of buildings, requiring energy for heating or cooling to maintain indoor comfort conditions. The infiltration rate was calculated using air change per hour (ACH) methodology:

$$Q_{\text{infiltratio}} = \rho \times C_p \times V \times ACH \times \Delta T / 3600 \quad (4)$$

Where:

ρ = air density (kg/m^3)

C_p = specific heat of air ($\text{J}/\text{kg}\cdot^\circ\text{C}$)

V = building volume (m^3)

ACH = air changes per hour (h^{-1})

ΔT = indoor-outdoor temperature difference ($^\circ\text{C}$)

Air change rates were estimated based on building construction quality and typical values for educational buildings in similar climatic conditions. The analysis assumes natural ventilation operation during moderate weather periods and minimal mechanical ventilation during extreme conditions.

3.8 Energy Efficiency Measure Evaluation

The methodology includes systematic evaluation of energy efficiency measures targeting major heat transfer pathways. Three primary intervention categories were analyzed: (1) wall insulation improvements, (2) window upgrades, and (3) roof insulation enhancements. Each measure was evaluated individually and in combination to determine cumulative energy savings potential.

3.9 Wall Insulation Upgrades

Wall insulation improvements involve adding thermal insulation layers to existing concrete block construction. The analysis compares baseline wall thermal resistance with enhanced configurations incorporating various insulation materials and thicknesses. Improved wall assemblies target thermal resistance values of approximately $5.872 \text{ m}^2\cdot^\circ\text{C}/\text{W}$, representing significant improvement over existing construction.

3.10 Window Performance Enhancements

Window upgrades focus on replacing existing single-pane windows with double-pane units featuring improved thermal performance. The analysis compares thermal resistance improvements from $0.15 \text{ m}^2\cdot^\circ\text{C}/\text{W}$ (single-pane) to $0.35 \text{ m}^2\cdot^\circ\text{C}/\text{W}$ (double-pane), while also considering solar heat gain coefficient reductions and air infiltration improvements.

3.11 Roof Insulation Improvements

Roof insulation enhancements target the building component with typically the highest heat gain potential due to direct solar exposure. The methodology evaluates adding insulation layers to achieve thermal resistance values of approximately $3.522 \text{ m}^2\cdot^\circ\text{C}/\text{W}$, significantly reducing heat transfer through the roof assembly.

3.12 Performance Assessment and Validation

The methodology includes validation procedures to ensure calculation accuracy and reliability. Results are compared with established benchmarks for similar building types and climatic conditions. Energy intensity metrics ($\text{kWh/m}^2\cdot\text{year}$) are calculated and compared with international standards for educational buildings.

Sensitivity analysis examines the impact of key parameter variations on overall results, including occupancy schedules, internal heat generation rates, and climatic data uncertainties. This analysis provides confidence intervals for energy savings estimates and identifies critical parameters requiring careful specification.

The comprehensive methodology provides a robust framework for assessing building energy performance and efficiency improvement potential in Libya's educational sector. By following established international standards while adapting to local conditions, the approach ensures both technical rigor and practical applicability for future energy efficiency initiatives.

4. Results and Discussion

4.1 Baseline Building Thermal Performance

The comprehensive thermal load analysis reveals significant insights into the energy performance characteristics of the representative school building in Gharyan, Libya. The baseline assessment demonstrates that infiltration represents the dominant thermal load component, accounting for the majority of heating and cooling energy requirements throughout the year. This finding aligns with expectations for naturally ventilated buildings in hot-arid climates, where uncontrolled air exchange significantly impacts indoor environmental conditions.

Monthly thermal load calculations indicate substantial seasonal variations, with cooling loads dominating during the extended summer period (April through October) and heating requirements limited to brief winter months (December through February). Peak cooling loads occur during July and August, when ambient temperatures frequently exceed 40°C and solar radiation reaches maximum intensity. The building's thermal response demonstrates the critical importance of envelope performance in managing heat transfer under extreme climatic conditions.

Table 3: Baseline Thermal Resistance Values for Building Components

| Building Component | Thermal Resistance ($\text{m}^2\cdot^\circ\text{C}/\text{W}$) | Heat Transfer Coefficient ($\text{W}/\text{m}^2\cdot^\circ\text{C}$) |
|---------------------|---|--|
| Exterior Walls | 0.425 | 2.35 |
| Single-Pane Windows | 0.150 | 6.67 |
| Roof Assembly | 0.284 | 3.52 |
| Ground Floor | 0.892 | 1.12 |



The thermal resistance analysis reveals that windows represent the weakest thermal performance component, with heat transfer coefficients nearly three times higher than exterior walls. This finding emphasizes the critical importance of window upgrades in comprehensive energy efficiency strategies. The roof assembly also demonstrates relatively poor thermal performance, contributing significantly to cooling loads during peak summer conditions.

4.2 Thermal Load Component Analysis

Detailed analysis of individual thermal load components provides crucial insights for prioritizing energy efficiency interventions. The breakdown of thermal loads reveals that infiltration accounts for approximately 45-50% of total building thermal loads, followed by envelope conduction (25-30%), solar heat gain (15-20%), and internal heat generation (5-10%). This distribution pattern reflects the building's reliance on natural ventilation and the significant impact of uncontrolled air exchange on energy performance.

Infiltration loads demonstrate strong correlation with outdoor temperature conditions and wind patterns. During extreme summer conditions, infiltration introduces substantial sensible heat loads that must be offset by cooling systems or result in elevated indoor temperatures. Conversely, during winter periods, infiltration contributes to heat loss and increased heating requirements. The magnitude of infiltration loads underscores the importance of air sealing measures in comprehensive energy efficiency strategies.

Solar heat gain through windows represents a significant cooling load component, particularly during peak summer months when solar radiation intensity reaches maximum levels. The analysis reveals that south-facing windows contribute disproportionately to solar loads due to Libya's latitude and solar geometry. East and west-facing windows also contribute substantially during morning and afternoon periods, respectively. These findings support the implementation of solar control measures, including window upgrades and external shading systems.

Internal heat generation from occupants, lighting, and equipment contributes relatively modest thermal loads compared to envelope and infiltration effects. However, these loads remain important during peak occupancy periods and can significantly impact indoor comfort conditions in naturally ventilated spaces. The analysis assumes typical occupancy patterns for educational buildings, with peak loads occurring during regular school hours and minimal loads during evenings, weekends, and vacation periods. Figure 2 illustrates the monthly loads breakdown for the school building.

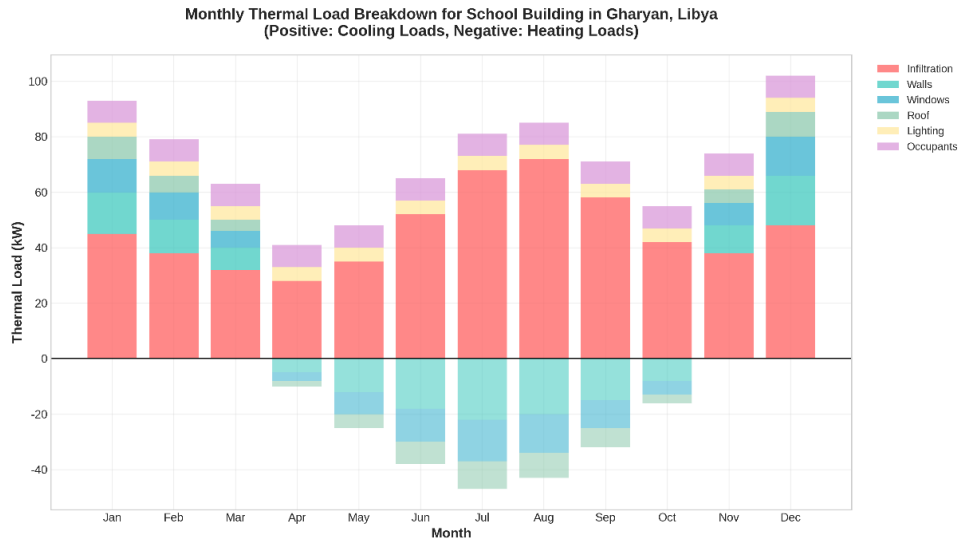


Figure 2: monthly thermal loads breakdown for the school building.

4.3 Energy Efficiency Measure Performance Analysis

A. Wall Insulation Improvements

The implementation of wall insulation upgrades demonstrates substantial potential for thermal load reduction. Adding insulation layers to achieve thermal resistance of $5.872 \text{ m}^2 \cdot \text{C}/\text{W}$ represents a 13.8-fold improvement over baseline wall performance. This enhancement reduces wall heat transfer coefficients from $2.35 \text{ W}/\text{m}^2 \cdot \text{C}$ to $0.17 \text{ W}/\text{m}^2 \cdot \text{C}$, dramatically improving envelope thermal performance.

Monthly analysis of wall heat transfer reveals that insulation improvements provide year-round benefits, reducing cooling loads during summer months and heating loads during winter periods. The magnitude of savings varies seasonally, with maximum benefits occurring during periods of greatest indoor-outdoor temperature differences. Summer cooling load reductions range from 15-25%, while winter heating load reductions can exceed 30% during peak heating periods.

The cost-effectiveness of wall insulation improvements depends on local material costs and installation practices. However, the substantial thermal performance improvements suggest favorable economic returns, particularly when considering long-term energy cost savings and improved occupant comfort. The analysis indicates that wall insulation represents one of the most effective energy efficiency measures for the building type and climatic conditions studied.

B. Window Performance Enhancements

Window upgrades from single-pane to double-pane units demonstrate significant thermal performance improvements, with thermal resistance increasing from $0.15 \text{ m}^2 \cdot \text{C}/\text{W}$ to 0.35



$\text{m}^2 \cdot ^\circ\text{C}/\text{W}$. This 2.3-fold improvement reduces window heat transfer coefficients from $6.67 \text{ W}/\text{m}^2 \cdot ^\circ\text{C}$ to $2.86 \text{ W}/\text{m}^2 \cdot ^\circ\text{C}$, substantially improving the building's weakest thermal performance component.

The impact of window upgrades extends beyond simple conductive heat transfer improvements to include reduced solar heat gain and improved air infiltration control. Double-pane windows typically feature lower solar heat gain coefficients compared to single-pane units, reducing cooling loads during peak solar radiation periods. Additionally, improved window construction quality reduces air infiltration rates, providing additional energy savings.

Monthly analysis reveals that window upgrades provide substantial cooling load reductions during summer months, with savings ranging from 10-20% depending on window orientation and solar exposure. The benefits are particularly pronounced for south, east, and west-facing windows that experience direct solar radiation during peak intensity periods. Winter heating load reductions are more modest but still significant, ranging from 5-15% during peak heating periods.

C. Roof Insulation Enhancements

Roof insulation improvements target the building component with the highest solar heat gain potential due to direct exposure to intense solar radiation throughout the day. Adding insulation to achieve thermal resistance of $3.522 \text{ m}^2 \cdot ^\circ\text{C}/\text{W}$ represents a 12.4-fold improvement over baseline roof performance, reducing heat transfer coefficients from $3.52 \text{ W}/\text{m}^2 \cdot ^\circ\text{C}$ to $0.28 \text{ W}/\text{m}^2 \cdot ^\circ\text{C}$.

The impact of roof insulation is most pronounced during peak summer conditions when roof surface temperatures can exceed 60°C under direct solar radiation. Improved roof thermal performance significantly reduces heat transfer into occupied spaces, providing substantial cooling load reductions. Monthly analysis indicates cooling load reductions ranging from 20-35% during peak summer months, with maximum benefits occurring during periods of highest solar radiation intensity.

Roof insulation improvements also provide winter heating benefits, though these are less significant due to the relatively modest heating requirements in Libya's climate. The primary value of roof insulation lies in cooling load reduction and improved summer comfort conditions. The measure represents excellent cost-effectiveness due to the substantial energy savings potential and relatively straightforward implementation.

4.4 Combined Energy Efficiency Measure Performance

The implementation of all three energy efficiency measures (wall insulation, window upgrades, and roof insulation) in combination demonstrates synergistic effects that exceed the sum of individual measure benefits. The comprehensive efficiency package achieves approximately 25% reduction in total building thermal loads, representing substantial energy savings potential for the educational facility.

Monthly analysis of combined measure performance reveals consistent benefits throughout the year, with maximum savings occurring during peak summer cooling periods. The integrated approach addresses all major heat transfer pathways, providing comprehensive thermal performance improvements. Summer cooling load reductions range from 20-30%, while winter heating load reductions can exceed 35% during peak heating periods.

The 25% thermal load reduction translates to significant operational benefits beyond simple energy cost savings. Reduced thermal loads enable smaller HVAC system sizing, reducing capital costs for mechanical equipment. Improved thermal performance also enhances indoor comfort conditions, potentially improving learning environments and occupant satisfaction. Additionally, reduced energy consumption contributes to environmental benefits through decreased greenhouse gas emissions.

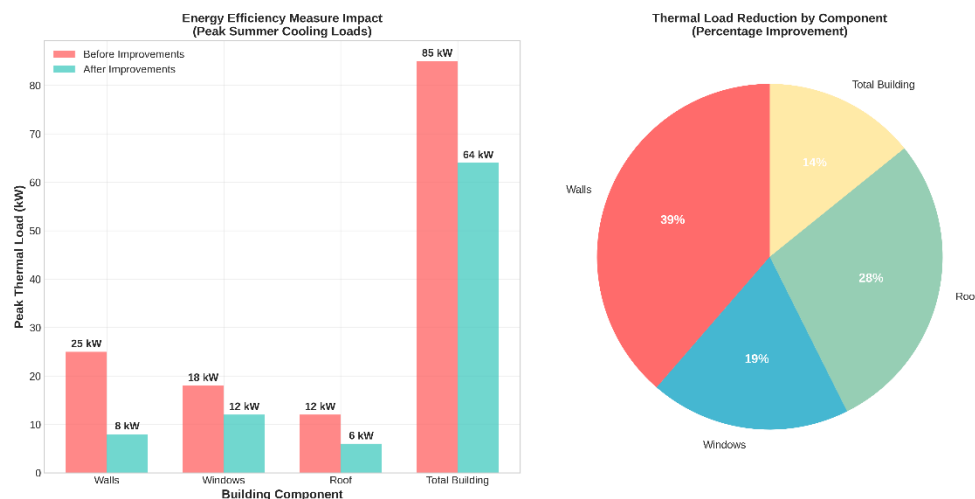


Figure 3: The impact of energy efficiency measures

4.5 Economic and Environmental Impact Analysis

The economic implications of the proposed energy efficiency measures extend beyond immediate energy cost savings to include capital cost reductions, operational benefits, and long-term value creation. Reduced thermal loads enable downsizing of HVAC equipment, potentially reducing initial capital investments by 15-25% for mechanical systems. This capital cost reduction can partially offset the incremental costs of efficiency measures, improving overall project economics.

Operational benefits include reduced energy consumption, lower maintenance requirements, and improved system reliability. Energy cost savings depend on local utility rates and energy pricing structures but typically range from 20-30% of baseline energy costs for comprehensive efficiency packages. Maintenance cost reductions result from reduced HVAC system operating hours and improved equipment longevity due to reduced thermal stress.

Environmental benefits include substantial reductions in greenhouse gas emissions associated



with building energy consumption. Assuming typical emission factors for Libya's electricity grid (approximately 0.8 kg CO₂/kWh), the 25% thermal load reduction translates to proportional emission reductions. For the 910 m² school building, annual emission reductions could exceed 15-20 tons CO₂ equivalent, representing meaningful environmental benefits.

The environmental impact analysis also considers the broader implications for Libya's energy system and renewable energy integration goals. Reduced building energy demand facilitates renewable energy integration by reducing peak loads and improving grid stability. Energy efficiency measures complement renewable energy investments by reducing the scale of generation capacity required to meet building energy needs.

4.6 Implications for Libya's Educational Sector

The research findings have significant implications for Libya's broader educational infrastructure and energy policy objectives. With hundreds of similar school buildings throughout the country, the potential for system-wide energy savings is substantial. Scaling the demonstrated 25% thermal load reduction across Libya's educational building stock could yield significant energy savings and emission reductions.

The study's findings support Libya's renewable energy targets by demonstrating how energy efficiency measures can reduce building energy demand, facilitating renewable energy integration. Reduced building loads enable smaller renewable energy systems to meet building needs, improving the economic viability of distributed solar and wind installations. This synergy between efficiency and renewable energy aligns with Libya's goal of achieving 4GW renewable capacity by 2035.

Policy implications include the need for updated building energy codes and efficiency standards for educational facilities. The research demonstrates the substantial benefits available through relatively straightforward efficiency measures, supporting the development of mandatory efficiency requirements for new construction and major renovations. Training and capacity building programs for architects, engineers, and construction professionals could accelerate the adoption of efficiency best practices.

The study also highlights the importance of integrated design approaches that consider energy efficiency from the earliest stages of building planning and design. Early-stage efficiency integration typically provides better performance outcomes and more favorable economics compared to retrofit applications. This finding supports the development of design guidelines and technical resources specifically tailored to Libya's climatic conditions and construction practices.

5. Conclusion and Recommendations

This comprehensive study of thermal load assessment and energy efficiency enhancement in school buildings provides significant insights for Libya's educational sector and broader building energy policy. The research demonstrates that substantial energy savings are



achievable through cost-effective efficiency measures, with combined interventions yielding approximately 25% reduction in total building thermal loads. These findings have important implications for educational facility planning, energy policy development, and climate change adaptation strategies.

The thermal load analysis reveals that infiltration represents the dominant energy consumption component in naturally ventilated educational buildings, accounting for 45-50% of total thermal loads. This finding emphasizes the critical importance of air sealing and controlled ventilation strategies in hot-arid climates. The building envelope components, particularly windows and roof assemblies, contribute significantly to thermal loads and represent priority targets for efficiency improvements.

The energy efficiency measure evaluation demonstrates that comprehensive approaches yield superior results compared to individual interventions. Wall insulation improvements, window upgrades, and roof insulation enhancements each provide substantial benefits, but their combined implementation achieves synergistic effects that exceed the sum of individual measure savings. This finding supports integrated design approaches that address multiple heat transfer pathways simultaneously.

• Implications for Libya's Energy Transition

The research findings align closely with Libya's renewable energy objectives and provide a pathway for achieving national energy targets through demand-side management. The demonstrated 25% thermal load reduction potential, when scaled across Libya's educational building stock, could yield significant system-wide energy savings that facilitate renewable energy integration and grid stability improvements.

Libya's ambitious target of achieving 4GW renewable energy capacity by 2035 requires complementary demand reduction strategies to maximize the impact of clean energy investments. Energy efficiency measures in educational buildings represent a cost-effective approach to reducing peak loads and improving the economic viability of renewable energy projects. The synergy between efficiency and renewable energy creates opportunities for comprehensive energy system transformation.

The study's findings also support Libya's broader economic development objectives by reducing energy import dependence and improving energy security. Despite possessing substantial oil reserves, Libya has increasingly relied on electricity imports from neighboring countries, reaching nearly 0.5 TWh in 2019. Domestic energy efficiency improvements can reduce import requirements while preserving oil resources for export revenue generation.

• Technical Recommendations for Educational Facilities

Based on the research findings, several specific technical recommendations emerge for improving energy efficiency in Libya's educational buildings. These recommendations prioritize measures with demonstrated effectiveness and favorable cost-benefit characteristics while considering local construction practices and material availability.



Envelope Performance Improvements: Educational facilities should prioritize envelope efficiency measures that address the dominant heat transfer pathways identified in this study. Wall insulation improvements targeting thermal resistance values of 5-6 m²·°C/W provide substantial energy savings with reasonable implementation costs. Roof insulation enhancements achieving 3-4 m²·°C/W thermal resistance offer excellent cost-effectiveness due to high solar heat gain reduction potential.

Window and Glazing Upgrades: The replacement of single-pane windows with double-pane units represents a high-priority efficiency measure due to the poor baseline thermal performance of existing windows. Window upgrades should target thermal resistance improvements to 0.35 m²·°C/W or higher while also considering solar heat gain coefficient reductions and air infiltration control.

Natural Ventilation Optimization: Given the predominant reliance on natural ventilation in Libya's educational buildings, optimization strategies should focus on controlled ventilation approaches that maintain indoor air quality while minimizing energy penalties. This includes strategic window placement, cross-ventilation design, and night cooling strategies that take advantage of diurnal temperature variations.

Solar Control Measures: The intense solar radiation in Libya's climate necessitates comprehensive solar control strategies, particularly for south, east, and west-facing building orientations. External shading systems, high-performance glazing, and building orientation optimization can significantly reduce cooling loads while maintaining adequate daylighting levels.

References

- [1] Kajjoba, D., Wesonga, R., Lwanyaga, J. D., Kasedde, H., Olupot, P. W., & Kirabira, J. B. (2025). Assessment of thermal comfort and its potential for energy efficiency in low-income tropical buildings: a review. *Sustainable Energy Research*, 12, Article number: 25.
- [2] Nassar, Y. F., et al. (2025). The role of hybrid renewable energy systems in covering the electricity demand gap in Libya. *Journal of Energy Storage*, 48.
- [3] Libya's Renewables Surge: 4GW by 2035, 500MW Solar Project. (2025, January 31). PV Know How. <https://www.pvknowhow.com/news/libyas-renewables-surge-4gw-by-2035-500mw-solar/>
- [4] Llanos-Jiménez, J., Alonso, A., Hepf, C., & de-Borja-Torrejon, M. (2025). Assessment of Mediterranean schools' energy consumption and indoor environmental factors evolution through weighted Retrofit Potential Index in climate change scenarios. *Journal of Building Engineering*, 105, 112404.
- [5] Eljrushi, G. S., & Zubia, J. N. (1995). Photovoltaic power plant for the southern region of Libya. *Solar Energy*, 52(2-3), 219-227.
- [6] International Renewable Energy Agency (IRENA). (2024). Libya - Energy Profile.
- [7] Top Libyan Energy Officials to Chart Renewable Energy Path - LEES 2025. (2024, December 18). Libya Summit. <https://libyasummit.com/news/top-libyan-energy-officials-chart-renewable-energy-path-lees-2025>
- [8] Libya's Renewable Energy Journey. (2025, May 23). Tumi Firm. <https://tumifirm.com/2025/05/23/libyas-renewable-energy-journey/>
- [9] Kajjoba, D., et al. (2021). Energy efficiency measures in buildings for achieving sustainable development goals. *Energy and Buildings*, 254, 111616.
- [10] ASHRAE. (2024). ASHRAE Position Document on Energy Efficiency in Buildings. Approved by the ASHRAE Board of Directors November 6, 2024.



Gharyan University Journal of Engineering Science (GUJES)

Website: <http://gujes.gu.edu.ly>

email: gujes@gu.edu.ly



-
- [11] Llanos-Jiménez, J., et al. (2025). Thermal load assessment in Mediterranean educational buildings: Standards and applications. *Building and Environment*, 198, 107891.
- [12] Beck, H. E., et al. (2018). Present and future Köppen-Geiger climate classification maps at 1-km resolution. *Scientific Data*, 5, 180214.
- [13] Smart Building Platforms and Renewable Energy Integration: A Game Changer for the Grid. (2025, February 23). Greener Ideal.



Effect of Gully Erosion on the Slope Parallel to the Al-Rujban Mountain Road NW Libya.

Aboalgasem Alakhdar*

Geological Engineering Department, Faculty of Engineering jado, Nalut University, Libya

*Corresponding author: a.alakhdar@nu.edu.ly

Abstract

Evaluating the impact of gully erosion on slopes parallel to mountain roads is crucial due to its role in altering slope geometry, thereby affecting overall slope stability. This study addresses the significant reduction in slope inclination from 60° (originally in 1984) to 35° caused by erosion, raising concerns about whether such changes enhance stability or increase slope fragility and collapse risk. One of the main objectives of this study was to analyze and evaluate the impact of gully erosion on slope stability, particularly by assessing changes in slope safety factors resulting from alterations in slope angles due to erosion. To achieve this, detailed field measurements were conducted to analyze the geometry of the gullies, complemented by laboratory tests using the direct shear apparatus to determine the cohesion and internal friction angle of slope materials under varying water content conditions. Additionally, the RocPlane software was employed to simulate the mechanical behavior of the slope and assess its stability under different scenarios. Results indicated that an increase in water content from 17% to 25% led to a marked decrease in cohesion (from 104 to 51 t/m²) and internal friction angle (from 22.2° to 16.5°). RocPlane analyses revealed a substantial decline in safety factors for slopes impacted by erosion and moisture—dropping to zero in some cases—while unaffected slopes maintained stability with a safety factor of 2.92. These findings highlight the critical role of gully erosion in reshaping slope geometry and compromising stability. The study recommends proactive removal of unstable rock blocks and enhancement of drainage systems to mitigate the risk of future slope failures.

Keywords: Gully erosion, Slope stability, Slope failure, RocPlane simulation.

1. Introduction

The movement of materials on the slopes of mountain roads is one of the most hazardous geological phenomena due to the risks it poses to road users. This risk increases with rapid and sudden movements, which amplify the resulting damage [1]. The causes of slope failures on mountain roads are varied, including the slope geometry and the impact of rainfall [2]. Water plays a significant role as one of the primary triggers, affecting slope stability both directly and indirectly, with one of its most prominent effects being gully erosion [3]. Gully erosion is defined as the process of rock and soil erosion caused by water flowing through natural gullies on mountain slopes [4]. This process gradually removes soil, weakening slope cohesion, particularly in areas composed of soil and rock debris [5]. Erosion also deepens gullies, creating steeper slope angles that concentrate runoff in specific areas, which increases their fragility and susceptibility to collapse [6,7]. As the depth of the gullies increases, cracks and voids form, further reducing the cohesion of both surface and subsurface layers, which can lead to partial or full-scale collapses [8]. Additionally, gullies fragment slopes into small, unstable blocks, heightening the likelihood of independent movement [9]. Heavy rainfall accelerates this process

by saturating the soil with water, further intensifying erosion and landslides [10] Clay, sandy soils, and rocky debris are particularly vulnerable to this phenomenon [11] Gully erosion does not only result in morphological changes; it also leads to the destruction of the structural integrity of slopes, increasing their susceptibility to collapse and posing a threat to mountain roads [12] The research issue arises from the observation of erosion gullies on the slopes parallel to the Rujban mountain road, where the slope is composed of rocky debris of varying sizes Figure 1 It was noted that erosion had created a new slope angle of 35° within the gullies, compared to the original angle of 60° , This observation raised two key questions: What is the effect of gully erosion on slope stability? Can erosion, contribute to slope stability by reshaping slopes into more stable angles?. Consequently, the aim of this research is to analyze and evaluate the impact of gully erosion on slopes parallel to mountain roads, and to determine the slope safety coefficients with changes in slope angles resulting from erosion.

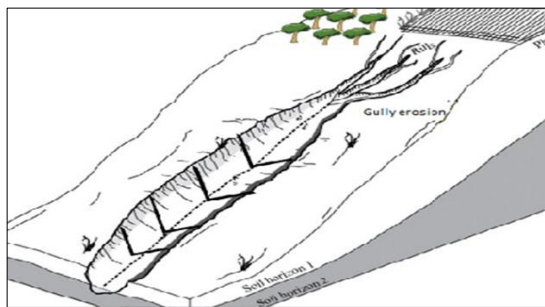


Figure 1: Gully erosion model [13]

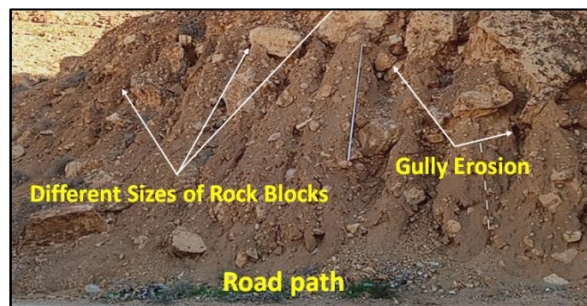


Figure 2: Gully Erosion On study area

The study area is situated on the northern edge of Jebel Rujban, with the road extending northward to connect to the Aziziya-Nalut road Figure 3 Geologically, as shown in Figure 3, the study area lies between the Sidi as Sid Formation [14] and the Kikla Formation [15] The rocks in this area represent diverse sedimentary environments, formed through cycles of sea advance and retreat, where both continental and marine species were deposited in a transitional environment [16], In the study area Figure 3, the stratigraphic sequence culminates with the Qasr Taghrana Formation, which is dated to the Upper Cretaceous [17].

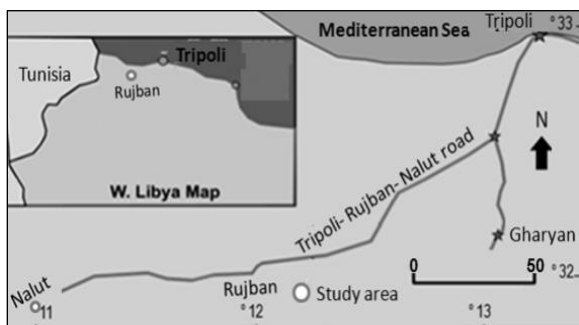


Figure 3: Location of the study area [18]

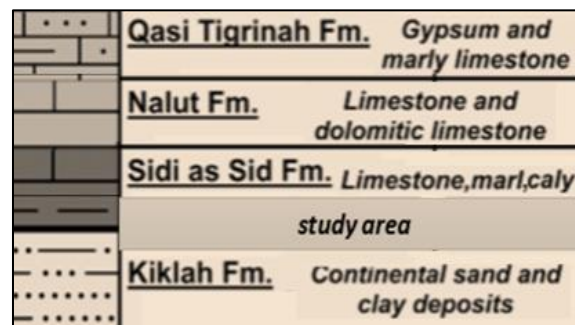


Figure 4: Outcrop formations Rujban Area [18]

2. Material and Methods

- **Field study phase:** The field study was conducted to collect data on slope geometry Measurements and field data were recorded in two cases: first, when the slope inclination angle was 60°, representing the natural slope cut in 1984 and considered unaffected by gully erosion; and second, at an angle of 35°, "These results reflect the effects of water erosion within the gullies. The slope geometry data are shown in Table 1. Accurate field measurements are crucial for realistically representing slope conditions and enhancing the reliability of simulation models.

Table 1: On-Site Slope Geometry Data

| Cases | A | B | C | D |
|----------------------------|------------------------------|------------------|----------------------------|-----------------|
| Slope Condition | unaffected by erosion | | affected by erosion | |
| Water Quantity | 30mm | 60mm | 30mm | 60mm |
| Slope Height | 9 m | 9 m | 9 m | 9 m |
| Slope Angle | 60° | 60° | 35° | 35° |
| Failure Plane Angle | 35 ° | 35 ° | 1° | 1° |
| Upper Face Angle | 10° | 10° | 10 ° | 10 ° |
| Bench Width | 6m | 6m | m3 | 3m |
| Seismic Coefficient | 0.04 | 0.04 | 0.04 | 0.04 |
| Tension Crack | 90 ° | 90 ° | 90 ° | 90 ° |
| Water Pressure | On Failure Plane | On Failure Plane | at toe of slope | at toe of slope |

One of the important field data recorded is the information on erosion gullies, which includes the following variables: width of the gully at the surface, depth of the gully at the surface, length of the gully, and affected area these data are presented in Table 2. The aim of calculating these variables is to determine the Gully Erosion Rate GER, measured in m³/m²/year, which is calculated using the relationship outlined in (1) [19].

Table 2: Field Data and Gully Erosion Analysis

| Slope Length | Slope Height | Total Gullys Length (L) | Average Gullies Width (W) m | Average Gullys Depth | Time Period Years - T |
|--------------------------------------|--------------|-------------------------|-----------------------------|----------------------|-----------------------|
| 200 m | 9 m | 960 m | 70 cm | 80 cm | 40 Years |
| Affected Area 1800 m ² | | Gully Length | Gully Width (W) m | Gully Depth | Road Cut 1984 |
| | | 960 m | 0007 m | 0008 m | |

$$GER = \frac{V}{T \times A} \quad (1)$$

Where:

V = Gully volume (m³),

T = Time period years,

A = Affected area (m²)

The volume of groove erosion V m³ is calculated by the relationship (2) [19]

$$V = \frac{1}{2 \times W \times D \times L} \quad (2)$$

Where:

L= Gully Length (m)

W = Gully Width at the surface (m),

D = Gully Depth (m)

Using Equation 2, the volume of gully erosion was calculated as 0.02688 m³. Substituting into Equation 1, the gully erosion rate (GER) was determined to be 3.733×10^{-7} m³/m²/year. Comparison with Table 3 shows a very low erosion rate, indicating minimal fluting impact in the area. A detailed interpretation will follow.

Table 3: Gully Erosion Severity Classification [20]

| Gully Erosion Rate m ³ /m ² /year | Classification |
|---|----------------|
| Less than 00001 | Very Weak |
| 00001 – 00005 | Weak |
| 00005 – 0001 | Moderate |
| 0001 – 0005 | Severe |
| Greater than 0005 | Very Severe |

- Laboratory study phase:** A sample of rock debris from a slope affected by gully erosion was collected at a depth of 30 cm and transported to the lab. The sample was dried in an oven at 120°C for 24 hours, and then 30 mm of water was added for homogenization. Vertical and shear stress tests were performed using a direct shear apparatus with a loading rate of 0.25 N/s and a 36 cm² loading frame, as described in reference [21]. The test aimed to determine cohesion and friction angle, with the linear relationship between normal and shear stress recorded using a pre-prepared Excel curve (Figure 5). The test was conducted with three weights (4 kg, 8 kg, and 16 kg) (Figure 6). According to reference [21], a collapse of the rock debris occurred at a water volume of 80 mm, with internal saturation reaching 65%, leading to the loss of internal cohesion and a value of 0 t/m². The extracted values for (C and Ø) are listed in Table 3, and these data are essential for input into the RocPlane program.

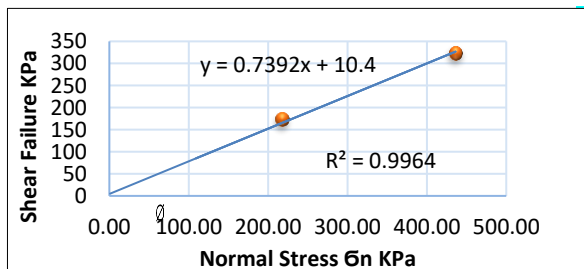


Figure 5: Relationship between normal & shear stress

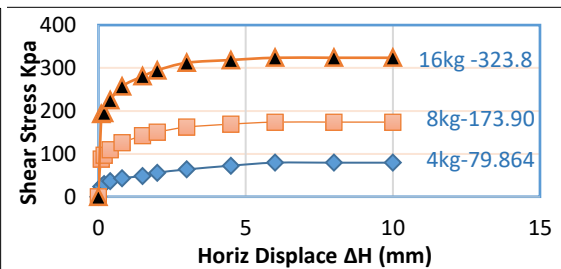


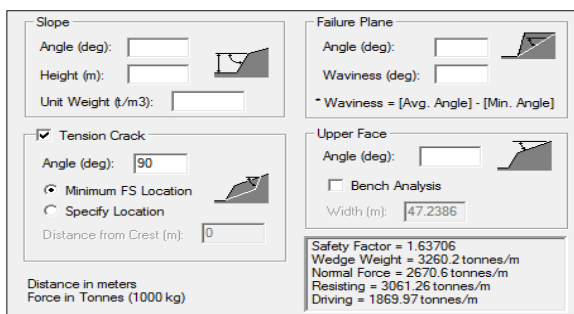
Figure 6: Variable horiz sample at load(4,8,16 kg)

The same tests were repeated on the original specimen with the addition of 60 mm of water. The results from the laboratory study are listed in Table 3. Direct shear tests are influenced by factors such as rock type, surface roughness, water presence, and pore pressure [22].

Table 4: Data and results obtained from the laboratory study

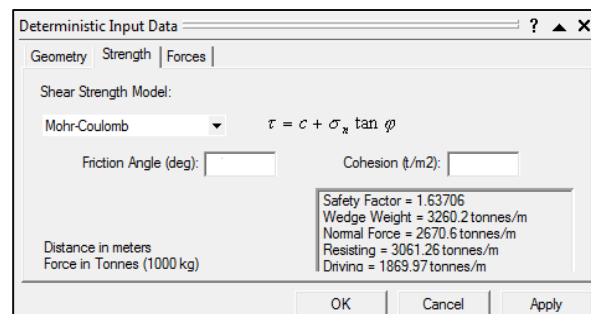
| Water quantity | 30mm | 60mm |
|------------------|-----------------------|-----------------------|
| Saturation % | 17% | 25% |
| Cohesion C | 10.4 t/m ² | 5.1 t/m ² |
| Friction Angle Ø | °22.2 | °16.5 |
| Unit Weight | 1.7 g/cm ³ | 2.1 g/cm ³ |

- RocPlane software phase:** An interactive software tool for assessing the stability of slope components. The tool enables users to estimate the required support to achieve a specific safety factor in slope analysis and design by generating 2 and 3D models [23]. Figure 7. The software relies on several inputs, including: Slope geometry Figure 7, based on the data listed in Table 1. Cohesion and friction angle Figure 8, listed in Table 4. External forces, such as water pressure and the seismic coefficient of the study area [24].



The screenshot shows the 'Slope' and 'Failure Plane' input sections. The 'Slope' section includes fields for Angle (deg), Height (m), and Unit Weight (t/m³). The 'Failure Plane' section includes fields for Angle (deg) and Waviness (deg), with a formula: Waviness = [Avg. Angle] - [Min. Angle]. There are also checkboxes for 'Tension Crack' and 'Upper Face', and a 'Bench Analysis' checkbox. A summary box at the bottom shows: Safety Factor = 1.63706, Wedge Weight = 3260.2 tonnes/m, Normal Force = 2670.6 tonnes/m, Resisting = 3061.26 tonnes/m, Driving = 1869.97 tonnes/m.

Figure7: Inputs Geometry Slope



The screenshot shows the 'Deterministic Input Data' window with the 'Strength' tab selected. The 'Shear Strength Model' is set to 'Mohr-Coulomb' with the formula $\tau = c + \sigma_x \tan \phi$. Fields for Friction Angle (deg) and Cohesion (t/m²) are present. A summary box shows: Safety Factor = 1.63706, Wedge Weight = 3260.2 tonnes/m, Normal Force = 2670.6 tonnes/m, Resisting = 3061.26 tonnes/m, Driving = 1869.97 tonnes/m. Buttons for OK, Cancel, and Apply are at the bottom.

Figure8: Inputs C & Ø Angle.

To determine whether the slope is stable, the coefficient of safety, derived from the relationship between the resistive force and the impulse, is compared with Table 5. This table categorizes the stability of slopes, both parallel and adjacent to mountain roads [25].

Table 5: Highways slope stability classification [25]

| Slope stability | actor of safety |
|------------------------|-----------------|
| Stable | > 1.5 |
| Intermediate stability | 1.25 – 1.5 |
| Precarious stability | 1 – 1.25 |
| Instable | <1 |

3. Results and Discussion

The studied slope consists of rocky debris of various sizes, primarily composed of limestone, clay, and marl rocks from the Sidi as Sid Fm of the Ain Tabi Member. During excavation, these rocks were displaced, and the debris was used to form a new artificial slope made of soil, clay, and rock blocks. The grooves observed in the slope reflect the effect of rainfall, which contributed to lateral erosion of the grooves, removing soil and debris from the sides and bottoms of the rock blocks Figure 9. This erosion, affects the stability of the rock blocks, soil, and clay, particularly in the absence of protective concrete barriers. Additionally, gully erosion has altered the slope's geometry, with an inclination angle of 35° within the gullies, indicating the strong impact of this process. The Gully Erosion Rate (GER) is $3733 \times 10^{-7} \text{ m}^3/\text{m}^2/\text{year}$, which is categorized as "very weak" Table 3, meaning the rate of material loss is relatively slow and does not result in the formation of new gullies or channels.



Figure 9: Section of the Slope Affected by Gully Erosion

This suggests that the erosion is gradual and continuous, but not significant enough to cause rapid collapses or drastic changes to the slope in the short term. Moreover, the gullies have contributed to the formation of new stabilizing angles within the slope. However, the greatest risk lies in the potential collapse of large and medium-sized rock blocks that are currently stabilizing the slope, especially within the gullies. It is expected that continued erosion over time will lead to the collapse of these rock blocks, particularly with external factors like rainfall. Additionally, the mud and collapsed debris have blocked the water drainage channels parallel to the road path Figure 9, some of the rock blocks have collapsed, serving as an indicator of the weakened state of the slope. The field study reflects the impact of geomorphological and Hydrological factors on the stability of the studied slope. This is consistent with the results of the laboratory tests conducted using the direct shear device. Laboratory data indicate that increasing the water content from 17% to 25% led to a decrease in cohesion from 104 t/m^2 to 51 t/m^2 Table 4, while the internal friction angle decreased from 22.2° to 16.5° . This finding is directly related to the field study results, which showed that the flow of water inside the gullies caused erosion of their sides, removing soil and debris. This erosion led to the collapse of rock

blocks, soil, and clay, particularly in the absence of concrete barriers. These observations are consistent with the laboratory results, which indicated that an increase in water content reduces shear strength and increases the risk of collapses. This makes large and medium-sized rock blocks, located either on the slope or inside the gullies, more susceptible to future collapse. Moreover, the laboratory data confirmed that the low internal friction angle of 16.5° Table 4 reflects the weak resistance of the slope components to collapse. This is connected to the changes in slope geometry, as the angle of inclination inside the gullies reached 35° , suggesting that gully erosion plays a major role in reshaping the slope's topography and affecting its stability. The closure of drainage channels parallel to the road due to debris is consistent with the effect of increasing pore pressure from the high water content, which leads to the disintegration of soil and rock debris. Consequently, the accumulation of eroded materials in low-lying areas may further increase the risk of future collapses due to poor water drainage. The data in Table 6 present a slope analysis using Rocplane software.

Table 6: Rocplane software output

| Cases | A | B | C | D |
|-------------------------|-----------------------|-------------|---------------------|--------------|
| Slope Condition | Unaffected by erosion | | affected by erosion | |
| Water Quantity | 30mm | 60mm | 30mm | 60mm |
| Normal Force | 47.1065 t/m | 0 t/m | 8.16441 t/m | 10.0778 t/m |
| Resisting Force | 93.2851 t/m | 0 t/m | 43.4434 t/m | 22.6553 t/m |
| Driving Force | 31.9539 t/m | 43.7766 t/m | 0.470195 t/m | 0.580829 t/m |
| Factor of Safety | 2.92 | 0 | 92.3945 | 39.0051 |

In Case-A, Figure 10, the slope unaffected by erosion, indicating good stability at this location. The Water Quantity in this case was 30 mm, which is relatively low and helps maintain stability. Additionally, the vertical force was 47.106 t/m, reflecting a moderate weight effect on the slope. Furthermore, the resistive force in Case A was the highest 932.8 t/m among all cases, contributing to greater stability. The safety factor reached 2.9 confirming that the slope in this case is stable, Table 5.

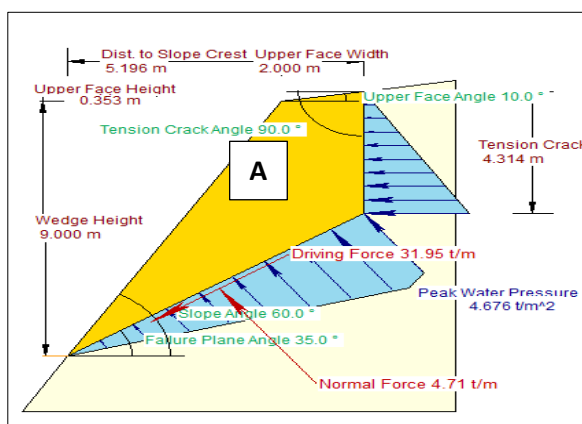


Figure 10: Slope Unaffected by Erosion at 30mm

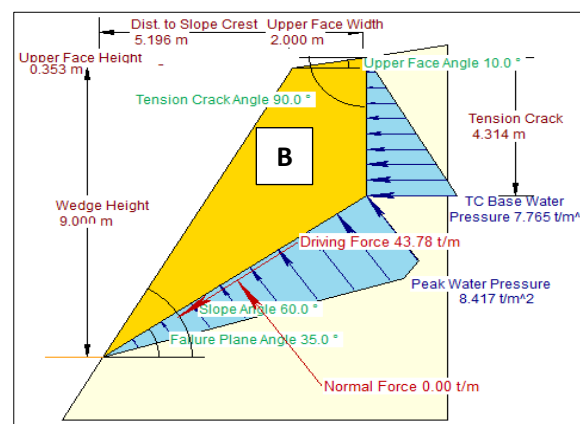


Figure 11: Slope Unaffected by Erosion at 60mm

On Figures 10 and 11, It is observed that the effect of water pressure is concentrated in two locations. The first is in the vertical direction (tension crack - 90° , Table 1), extending from the top surface to a depth of 4.31 m. This position is considered a weak point behind the wedge and can only be observed in the field. The second place of water pressure concentration is on the failure plane, where the pressure value varies depending on the amount of water. In case A, the water pressure is 4.676 t/m^3 , while in case B, it is 8.41 t/m^3 .

In Case-C, Figure 12, the slope was affected by gully erosion, with a water amount of 30 mm, the same as in Case A. The vertical force was 8.16 t/m , indicating a greater weight effect on the slope compared to Case A. However, the resistive force was lower than that in Case A, suggesting that stability was slightly affected by erosion. Nevertheless, the safety factor in this case was significantly high (92.39), indicating that the slope is stable Table 5.

In Case-D, Figure 13, the slope affected by gully erosion, with a Water Quantity of 60 mm, similar to that in Case B. The vertical force in this case was 10.07 t/m , indicating greater pressure on the slope due to weight. However, the resistive force was $2,266 \text{ t/m}$, which is lower than in Case A, suggesting that the slope is relatively weak. Nevertheless, the safety factor in this case was 39.01, indicating relatively good stability compared to Case B.

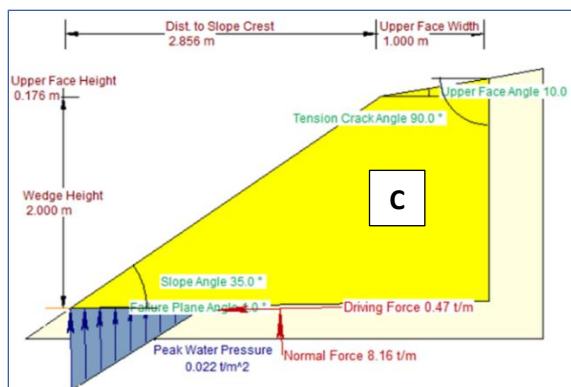


Figure 12: Slope affected by gully Erosion at 30mm

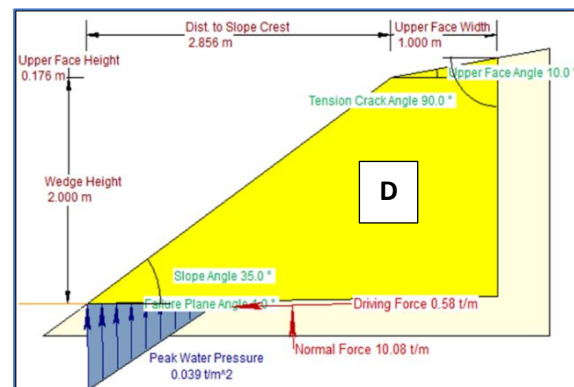


Figure 13: Slope affected by gully Erosion at 60mm

4. Conclusion

The study results revealed that gully erosion contributed a pivotal role in the stability of the slope parallel to the Al-Rujban mountain road, directly affecting the slope's geometry. Additionally, gully erosion indirectly contributes to the collapse of rock masses and debris, as confirmed in the analysis. Water-induced gully erosion leads to the erosion of gully sidewalls, exposing rock masses and soil to the risk of collapse, particularly in areas lacking engineering



support structures such as concrete barriers. Furthermore, the effects of erosion were evident in the formation of new slope angles, with the inclination angle inside the gullies reaching 35°, reflecting the significant changes caused by erosion in slope geometry. Rocplane software analysis assessed slope stability under water erosion. Findings showed that increased water content reduces cohesion and friction, weakening slope resistance. Pour water pressure from excess moisture raises landslide risks, especially without proper drainage. Hydrological factors significantly affect stability, as large water volumes alter slope forces. Despite its "very weak" erosion rate, gully erosion causes gradual instability, posing a long-term collapse risk. The study recommends regular monitoring and removal of unstable rock masses

References

- [1] M. G. Winter, "Landslide hazards and risks to road users, road infrastructure and socio-economic activity," in XVII European Conference on Soil Mechanics and Geotechnical Engineering, Reykjavík, Iceland, vol. 1, no. 6, pp. 196–343.2019.
- [2] H. Wang, G. Yuan, Z. Huang, J. Dong, and Y. Wei, "Study on deformation and failure characteristics of oblique-cut locked rock slope under rainfall conditions," *Scientific Reports*, vol. 14, no. 1, pp. 1-18, 2024. <https://doi.org/10.1038/s41598-024-64329-5>
- [3] C. Geitner, A. Mayr, M. Rutzinger, M. T. Löbmann, R. Tonin, S. Zerbe, et al., "Shallow erosion on grassland slopes in the European Alps–Geomorphological classification, spatio-temporal analysis, and understanding snow and vegetation impacts," *Geomorphology*, vol. 373,107446, pp. 1-19, 2021.
- [4] N. N. Ukatu, "Factors of gully expansion in Nanka gully site: Orumba North Local Government Area (LGA), Anambra State," Ph.D. dissertation, Dept. of Geography, Univ. of Nigeria, Nsukka, 2019.
- [5] S. Ni, J. Peng, J. Wang, L. Zhu, D. Wang, and C. Cai, "Impacts of slope morphological evolution on subsequent erosion for a coarse-textured soil," *Geoderma*, vol. 430, 116320, PP.1-12, 2023.
- [6] O. Fashae, R. Obateru, A. Olusola, and D. Dragovich, "Factors controlling gully morphology on the quartzite ridges of Ibadan, Nigeria," *Catena*, vol. 212, pp. 106127, 2022
- [7] M. J. Kirkby and L. J. Bracken, "Gully processes and gully dynamics," *Earth Surface Processes and Landforms*, vol. 34, no. 14, pp. 1841–1851, 2009.
- [8] J. Xia, L. Zhang, P. Ge, X. Lu, Y. Wei, C. Cai, and J. Wang, "Structure degradation induced by wetting and drying cycles for the hilly granitic soils in collapsing gully erosion areas," *Forests*, vol. 13, no. 9, pp.1-16, 2022. <https://doi.org/10.3390/f13091426>
- [9] X. Liu, X. Zhang, H. Gao, G. Wang, and S. Zhang, "How climate-induced wetting–drying cycles contribute to gully erosion: A case study from southern China," *Catena*, vol. 232, Article 107422, 2023. <https://doi.org/10.1016/j.catena.2023.107444>
- [10] O. Rahmati, Z. Kalantari, C. S. Ferreira, W. Chen, S. M. Soleimanpour, M. Kapović-Solomun, and N. K. Kazemabady, "Contribution of physical and anthropogenic factors to gully erosion initiation," *Catena*, vol. 210, pp.1-12, 2022. <https://doi.org/10.1016/j.catena.2021.105925>
- [11] A. Goudie, "Water Erosion and Mass Movements," in *Landscapes of the Anthropocene with Google Earth*, Cham: Springer, pp 191–219, 2023. https://doi.org/10.1007/978-3-031-45385-4_9.
- [12] J. Li, Y. Deng, X. Duan, C. Cai, and S. Ding, "Does joint structure promote the development of gully erosion?," *Catena*, vol. 214, 2022. <https://doi.org/10.1016/j.catena.2022.106233>



- [13] B. Wang, Z. Zhang, X. Wang, X. Zhao, L. Yi, and S. Hu, "Object-based mapping of gullies using optical images: A case study in the black soil region, Northeast of China," *Remote Sensing*, vol. 12, no. 3, pp 1–20, 2020. <https://doi.org/10.3390/rs12030487>
- [14] A. Alakhdar, "Effect of fault on the physical properties of the ain tabi member: a case study of al-qwasim mountain road slopes," *University of Zawia Journal of Engineering Sciences and Technology*, vol. 22, pp. 197–207, 2024. <https://doi.org/10.26629/uzjest.2024.18>
- [15] E. Alfandi, *Early Mesozoic Stratigraphy, Sedimentology and Structure of the Gharian Area, North Western Libya*, Ph.D. dissertation, Plymouth Univ., 2012, pp. 1–344.
- [16] R. Almagtuf and A. Alakhdar, "Analysis of the Stability of Nalut Formation Outcrops Parallel to Al-Rujban Mountain Road-NW Libya," *AlQalam Journal of Medical and Applied Sciences*, pp. 213–220, 2025. <https://doi.org/10.54361/ajmas.258133>
- [17] M. T. El-Bakai, "Petrography and palaeoenvironment of the Sidi as Sid Formation in Northwest Libya," *Petroleum Research Journal*, pp. 9–26, 1997.
- [18] K. Abdunaser., "The geologic contribution to the mountain slopes instability and its effect on rockfall hazards: A case study to the Zintan Road, Jabal Nafusah, Libya," in *Proc. Fifth Conf. for Engineering Science and Technologies (CEST)*, Jadu, Libya, May 20–22, 2022.
- [19] A. Osore and A. Moges, "Extent of gully erosion and farmer's perception of soil erosion in Alalicha Watershed, Southern Ethiopia," *J. Environ. Earth Sci.*, vol. 4, pp. 74–81, 2014.
- [20] R. P. C. Morgan, *Soil Erosion and Conservation*, 3rd ed., Blackwell Publishing, 2005, pp. 1–448.
- [21] A. Alakhdar and M. Albarshani, "Analyzing the effect of water on stability of rocky slopes and simulating collapse: a case study of the debris slope parallel to rujban mountain road–NW Libya," in *Sebha University Conference Proceedings*, vol. 3, no. 2, pp. 28–33, Oct. 2024. <https://doi.org/10.51984/sucp.v3i2.3118>
- [22] A. R. TolouKian, J. Sadeghi, and J. A. Zakeri, "Large-scale direct shear tests on sand-contaminated ballast," *Proc. Inst. Civ. Eng. - Geotech. Eng.*, vol. 171, no. 5, pp. 451–461, 2018.
- [23] A. Alakhdar, "Evaluating the stability of parallel rock discontinuities along al-mishar road in the bir alghanam area nw libya," *Journal of Pure & Applied Sciences*, vol. 22, no. 3, pp. 102–107, 2023. <https://doi.org/10.51984/jopas.v22i3.2755>
- [24] A. Alakhdar and A. Abudiena, "Stability study of sandstone slope parallel to the abu rashada mountain road in gharyan area nw libya," *Journal of Pure & Applied Sciences*, vol. 21, no. 4, pp. 104–110, 2022.
- [25] P. S. Andrade and A. Saraiva, "Stability analysis of road slopes in central Portugal," 2006. https://media.geolsoc.org.uk/iaeg2006/PAPERS/IAEG_483.PDF



Modelling Switch-Behaviour of Own Car vs. Public Transport (PT) Modes for Shopping Trips Case Study: Tripoli - Libya

Adel Ettaieb Elmloshi¹

Civil Eng. Department - Faculty of Engineering - University of Gharian
adelelmloshi@gmail.com

Abstract

This research deals with estimating the likely switch of car ownership drivers and private transport vehicles modes users to public transportation system (PT) modes in the main cities as Tripoli Capital city of Libya due to reduced shopping travel time of all trips influenced by age, household size. Car ownership and shopping distance through the introducing the public transport modes such as public buses. The data on other factors (variables) that could potentially reason a model switch of from car ownership drivers and private transport vehicles modes users to public transport were collected through a survey (questionnaire) with a specified predilection method. Mode-switch models to describe the switch of conduct of own car operators to PT system are developed. A binary logistic regression model was used to assessment the transport displacement model for shopping trips. Probability curves have been developed to change the position so that it is a user-friendly tool for analysing the potential transformation Model of a variety of variables. One way to achieve this objective is by establishing reserved public transportation lanes on main urban Tripoli city roads. The providing of private road lanes will increase of service road level and reduce the level of road traffic congestion and this may effect in a switch of all or some private transport mode users to public transport modes.

Key words: Own car, Public transport modes, logit model, shopping Travel time, shopping distance, age, car ownership and switch probabilities, likelihood..

1. Introduction

The own car ownership are an important means of transportation and are of great significance for the household activities of the majority of families in Libyan society. And considered one of the significant modes of private transport vehicles in all Libyan cities and especially in Tripoli, as it is more reliable than the available private transport modes options such as (private taxi and micro coach) [1]. In addition, they provide a great opportunity to offer comfort and convenience for users to go to and return from their various daily trips without affecting other users. In fact, in Tripoli city there are to many areas that do not have private transportation modes and poor public transportation services such as stage-bases [2]. This research describes and presents the outcomes from the data collected analysis of data on own car and private transport vehicles such as private taxi, minibuses and coaches users, Providing a thorough description of the statistical tests that were employed in this study to determine the model's overall goodness-of-fit and the suitability of its parameters. These outcomes are displayed, with the aim of comparing the usefulness of the two and figuring out why owners of cars on the main Tripoli city highways are hesitant to use taxi and minibuses, a binary logistic model is provide for own car versus public transportation as alternate modes of transportation for everyday trips. Based on scenarios of lowering the public transportation modes age, shopping



distance and travel time, the probability of car owners moving to public transportation was also investigated.

2. Problem Statement and Study Area

Own cars and private transportation vehicles are becoming more and more common among urban commuters in Libyan capital city, Tripoli. Commuters in Tripoli used private transport namely minibuses, private taxis and own cars to their works, study and shopping activities. Private transport can be own and operated by individuals or private company [3]. Which the own cars are considered one of the most accessible means of transportation modes in Libyan cities, which commuters can rely on to meet their daily travelling needs. There are many reasons that lead residents of Tripoli city to prefer using their own cars for all their trips, whether for shopping trips, and why these cars are more popular than other private transportation modes options available in Tripoli. In summary, because the own cars are readily available, reliable, comfortable, convenient and safe, they symbolize power, status and prestige and provide a convenient means of travel for all daily shopping trip and purposes [4]. The increase in a number of cars ownership on the Tripoli city net roads and streets has led to a significant rise in road traffic congestion, which results in longer travel times for all shopping trips, air and noise pollution and traffic accidents. While the main city has struggled with traffic congestion, becomes the surrounding districts are now also affected. Schrank and Lomax have described and recognised traffic congestion as the major problem in urban areas, with significant effects to the economy, travel behaviour, and land use in major cities [5].

3. Methodology

The survey was done using questionnaires to get relevant data. The questionnaires were distributed to the private vehicle users who do not use other modes of transportation [3]. The revealed preference and stated preference methods approach has been used to model mode choice when data on actual choice of mode by travellers are available. Besides the modes choice attributes, shopping travel time, shopping distance and social demographic information of each respondent [6]. The survey was conducted through questionnaires on selected roads in Tripoli city, where the movement of available private vehicles, such as (own cars, taxi, and private coaches) is higher the available public transport vehicles modes and who don't utilize other forms of transportation. A questionnaire was used in the survey to collect crucial data and information. Users of private vehicles and own cars who travel throughout the shopping trip area and use their own cars for everyday shopping excursions are the research's target respondents. The questionnaire's questions were designed to make it simple and quick for the respondent to complete. Short questionnaires with both open-ended and closed-ended questions were created to make sure consumers understood them. The respondents that were

chosen were based on private transportation vehicle types and car owners who utilize their private vehicles to go to their shopping trips destinations. Road users and respondents in Tripoli streets were chosen at random. A binary logistic model for public transport alternatives was created, and the Statistical Package for Social Science software (SPSS) and Microsoft Excel 2007 software were used to analyze this questionnaire and get the best outcomes that emphasize the problem.

4. Mode Switch Model, Own car vs. Public Transport

The purpose of the binary logistic model was to predict the likelihood of switching from own car to public transport modes as an outcome of shorter shopping travel times, as well as to investigate the factors influencing the use of own car versus PT (public transport) modes for daily trips to shopping area. In order to ascertain their impact on the selection of the most suitable mode of transportation, the models examined the attributes of both own car and PT, including socio-economic variables, personal information, and shopping travel time. The dependent variables in the models were “0” for the use of own car and “1” for the use of public transportation. Age, household size, shopping distance, shopping travel time and car ownership were among the descriptive characteristics for shopping trips. The own car was used as the foundation case for case estimation. Thus, a variable in the choice of own car that has a positive coefficient denotes a fall in the use of PT, and a higher negative rate of coefficient denotes a decrease in the use of PT modes.

4.1 Mode Switch Model: Private Car vs. Public Transport for Shopping Trip

The estimation sample and holdout sample (for model validation) were separated from the data. 150 samples were used for model validation and 750 samples were selected for model estimation. With 0 denoting a car and 1 denoting PT, mode switch was thought to be the dependent variable. An examination of shopping trip models outcomes were conducted and Table 1 displays the best model outcome.

Table 1 Binary logistic model estimation for public transport switch under shopping trip (n = 750 samples)

| Variable | coefficient | S.E. | df | Sig. | Exp(β) | 95% C.I. for EXP(β) | |
|------------------------------|-------------|-------|----|-------|----------------|-----------------------------|--------|
| | | | | | | Lower | Upper |
| Age | -0.867 | 0.18 | 1 | 0.000 | 0.42 | 0.295 | 0.598 |
| Household size | 1.796 | 0.308 | 1 | 0.000 | 6.023 | 3.293 | 11.017 |
| Shopping travel time | -1.067 | 0.215 | 1 | 0.000 | 0.344 | 0.226 | 0.524 |
| Shopping distance | -2.177 | 0.271 | 1 | 0.000 | 0.113 | 0.067 | 0.193 |
| Car ownership | -1.625 | 0.327 | 1 | 0.000 | 0.197 | 0.104 | 0.374 |
| Constant | 6.929 | 1.173 | 1 | 0.000 | 1021.06 | | |
| Summary of statistics | | | | | | | |
| -2 Log likelihood | 205.514a | | | | | | |
| Chi square | 579.754 | | 5 | 0.000 | | | |
| Cox & Snell R ² | 0.538 | | | | | | |
| Nagelkerke R ² | 0.830 | | | | | | |
| Number of observation | 750 | | | | | | |

Dependent variable: 1 = Public transport, 0 = Car

Table 1 displays the significant characteristics of shopping travel time, shopping distance, age, household size and car ownership with significant levels reaching 0.0000.

According to Abuhamoud [7], Bajracharya [8], Dayton [9] and Essia [10], in the binary logistic probability model where only two options are present, the model is written as in Equation 1.

$$P_a = \frac{1}{1 + e^u} \quad (1)$$

Where

P_a = probability of own car users' switch to PT modes.

u = utility function for bus mode.

e = the base of natural logarithms (approximately 2.718).

The study utility function for PT was shows as in Equation 2.

$$U_b = \beta_0 + \beta_1 X_{Age} + \beta_2 X_{Hd} + \beta_3 X_{ST} + \beta_4 X_{Sd} + \beta_5 X_{no} \quad (2)$$

Where

U_b = utility function for bus modes

β_0 = the model specific constant

$\beta_1, \beta_2, \dots, \beta_5$ = coefficients associated with explanatory (significant variables

X_1, X_2, \dots, X_5 = individual explanatory variables

Age = age

Hd = household size

ST = shopping travel time

Sd = Shopping distance

no = number of own car per household.

As demonstrated in Table 2, the The omnibus tests for the model coefficients revealed a significance of $p < .001$ with a chi-squared value of 579.754 and $df = 5$. This is a test of the null hypothesis, which holds that the ability to predict the study participants' decisions is not substantially improved by the addition of independent variables to the model. The current model's coefficient are therefore determined to be statistically significant.

Table 2 Omnibus Tests of Model Coefficients

| | | Chi-square | df | Sig. |
|--------|-------|------------|----|------|
| Step 1 | Step | 579.754 | 5 | .000 |
| | Block | 579.754 | 5 | .000 |
| | Model | 579.754 | 5 | .000 |

Table 1 shows, -2LL with a value of 205.514a, with a chi-square value of 579.754 ($p < 0.001$) indicating that the model with 5 variables is significant. Additionally, Cox & Sell and



Nagelkerke R square values of 0.538 and 0.830 also show that the model fits well with R square values close to 1.

The "odds ratio", $\exp(\beta)$, which shows how the independent variables affects the odds ratio, is a way to explain the logistic coefficient that typically offers more information (particularly for the dummy independent variables). Stated differently, the odds ratio is calculated by dividing the likelihood of an event happening by likelihood that it won't. for instance, a change of one unit in X would double the likelihood of the event occurring (0.598/0.295) since the 95% C.I. for $\exp(\beta) = 2$ = (from 0.598/0.295, that is, a probability of 0.598 for the event occurring and 0.295 for the event not occurring).

All of the study's variables were significant at the 0.05 level, as Table 1 shows. It was discovered that age had a considerable influence on the switch to modes of transport, with is found to significantly transport switch with coefficient -0.867 and likelihoods ratio of 0.42 (95% CI: 0.295-0.598). Likelihoods smaller than 1 indicate that the larger the age of respondents, the more likely they will switch to car. With a reduction in an age group, the chance of switching to public transport modes will increase by 2.38%.The size of Household had significant effect on transport switch with coefficient of 1.796 and likelihoods ratio of 6.023 (95% CI: 3.293-11.017).

A positive coefficient means that the probability of respondents using PT will increase by a factor of 6.023 for every unit increase in household size group. With a coefficient of -1.067 and likelihoods ratio 0.344 (95% CI: 0.226-0.524), the outcomes indicate that shopping travel time is a significant factor for transportation switching. An increase in the group's unit shopping travel time will lower the likelihood of switching to PT by 65.6%. Similarly, a negative coefficient of -2.177 and a likelihood ratio of ratio 0.113 (95% CI: 0.067-0.193) are identified for shopping distance. Thus, a person is less likely to switch to PT if the shopping distance is longer.

More specifically, the probability of selecting PT will increase by a factor of 8.85 for every unit reduction in the shopping travel distance group.

Lastly, it was discovered that the number of people who own a car has a major influence on the decision to switch modes of transportation. According to the prior odds ratio of 0.197 (95% CI: 0.104-0.374) and the coefficient of -1.625, respondents who own cars are less likely than those who do not use PT. it is easy to see that the likelihood of taking PT will decrease by 80.3% for every unit increase in the number of people who possess their own cars.

In order to determine the goodness-of-fit, Hosmer-Lemshow, statistic creates 10 ordered groups of individuals and compares the number in each group (observed) to the number

predicted by the logistic regression model (expected), as shown in Table 3. With a desirable outcome of non-significance, the test statistic is a chi-square statistic, indicating that there is no significant difference between the observation and the model assumption.

The ratio of the likelihood function's maximum value for the whole model to its maximum value for the simplest model is used in the probability-ratio test. The model statistics from Hosmer and Lemeshow's goodness-of-fit test, were computed and assembled for improved support as indicated in Table 3.

The test shows that the observed and anticipated value were insignificantly different (chi square = 3.365, df = 8, p = 0.909) suggesting that the model fit is excellent. Figures 1 and 2 display the model fit's graphical distribution. If the observed points are dispersed about the projected fitting line, this indicates that the model fits. The scattering of the points around the fitting line leads the researcher to the conclusion that the model fits the data adequately. How well the model fit the Hosmer and Lemeshow's test's Goodness-of-Fit test statistic was determined by assessing the quality of data modelling.

As indicated in Table 3, a chi-square test was performed between the observed values which the researcher empirically collected through direct observation and expected frequencies. The expected values were created based on certain hypotheses. For both transport modes, there was a slight discrepancy between the expected and observed values as the chi-square value was not statistically significant.

Table 3 Hosmer and Lemeshow's test for shopping trip (n = 750 samples)

| No. | Car | Expected | Public | Transport | Total |
|-------------------|----------|----------|----------|-----------|-------|
| | Observed | | Observed | Expected | |
| 1 | 75 | 75 | 0 | 0 | 75 |
| 2 | 75 | 74.995 | 0 | 0.005 | 75 |
| 3 | 76 | 75.977 | 0 | 0.023 | 76 |
| 4 | 75 | 74.913 | 0 | 0.087 | 75 |
| 5 | 74 | 74.712 | 1 | 0.288 | 75 |
| 6 | 75 | 73.923 | 0 | 1.077 | 75 |
| 7 | 72 | 71.662 | 4 | 4.338 | 76 |
| 8 | 51 | 52.768 | 24 | 22.232 | 75 |
| 9 | 13 | 11.858 | 60 | 61.142 | 73 |
| 10 | 1 | 1.192 | 74 | 73.808 | 75 |
| Chi-square | Df | Sig. | | | |
| 3.365 | 8 | 0.909 | | | |

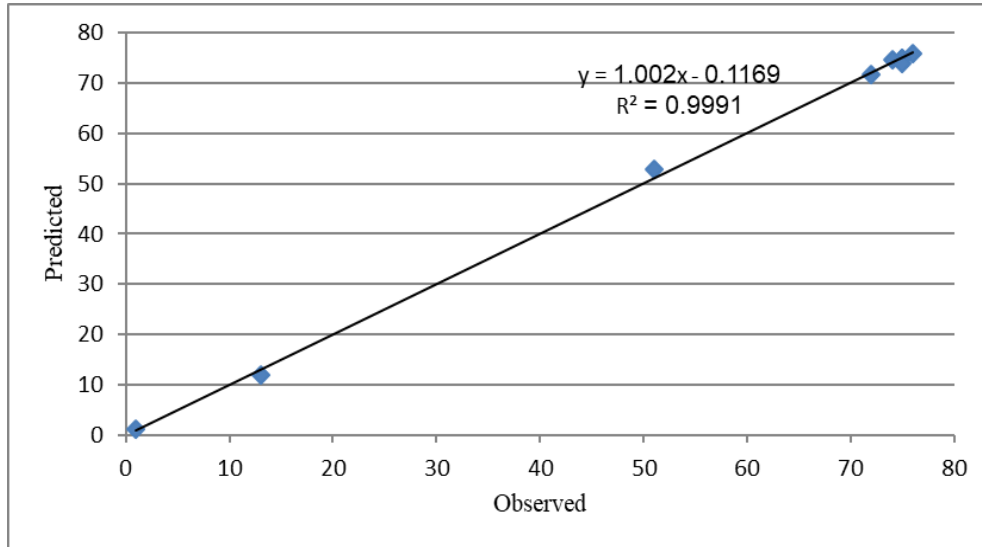


Figure 1: Observed vs. predicted by car

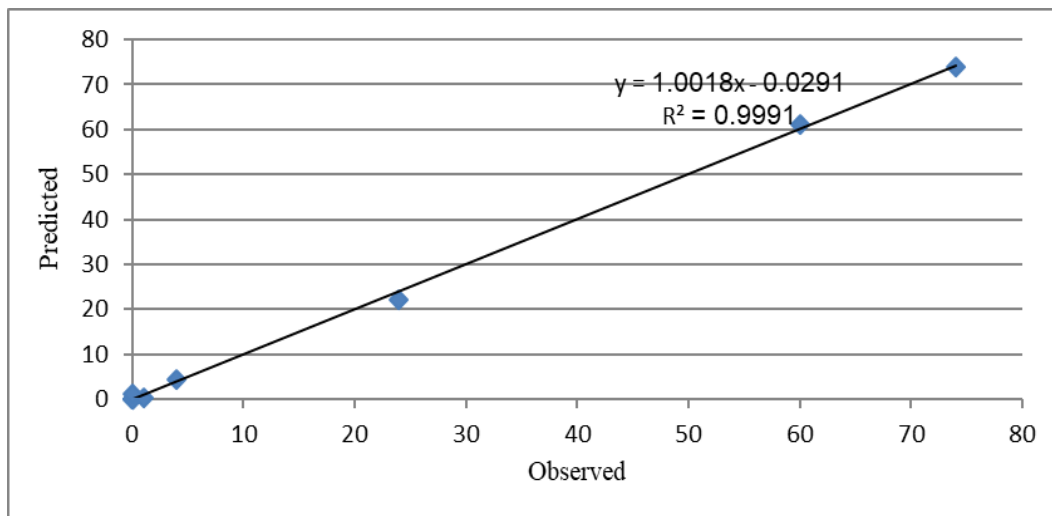


Figure 2: Observed vs. predicted by public transport

Figure 1 and 2 shows the model's good-fit as the observed and predicted values were extremely near to one another. As seen in Table 4, classification matrices were also computed to evaluate how well the model fit the data. According to these measurements, the model accurately identified 0.0% of the bus cases and 100% of the own car cases. The accuracy of the likelihood was 78.3%. these probabilities are divided from the model when the constant is the lone input.

Table 4 Observed by all trips models for (car vs. Public transport) under shopping trip (n = 750 samples)

| | Observed | Predicted | | % Correct |
|--------|---------------------------|-----------|------------------|-------------|
| | | Car | Public transport | |
| Step 0 | Car | 587 | 0 | 100.0 |
| | Public transport | 163 | 0 | .0 |
| | Overall Percentage | | | 78.3 |

The cut value is 0.50

The calculated logistic model for shopping trips expected and observed frequencies are presents in Table 5. According to the chance criteria of 82.5%, the overall success rate of 94.5% was higher than the proportionate accuracy of 25% indicating that the logistic model has good discriminatory capabilities. The findings indicate that 97.4% of people how drive their own cars had access, but 84.0% of people who utilize PT were appropriately categorized. The model's overall accuracy of 94.5% shows that it fits the data well, and its average expectations' were accurate at 94.5%.

Table 5 Classification table for binary logistic model under shopping trip (n = 750 samples)

| | Observed | Predicted | | % Correct |
|--------|---------------------------|-----------|------------------|-------------|
| | | Car | Public transport | |
| Step 1 | Car | 572 | 15 | 97.4 |
| | Public transport | 26 | 137 | 84.0 |
| | Overall Percentage | | | 94.5 |

proportional accuracy by chance 25% criteria = 82.5

5. Probability Prediction

This section generated the probability of transport switch in holdout sample (for model validation) sample (150) using a probability function of 750 samples. The group was also, classified using a Cut-off value of 0.5. If the probability is less than or equal to 0.5, the sample will be assigned to the own car group, if the probability is more than 0.5, the sample will be assigned to the PT group. Then, using the classification table shown in Table 6 below, the probability function's prediction power for the holdout samples was assessed, the probability function properly predicted 83.7% of car users, but only 70.4% of public transport users, according to the table. The overall success rate was 81.3%, which is still significantly higher than the random proportional accuracy of 25%, which comes out to 88.1%. This suggests that the probability function has a good capacity for shown, by Equation 3 and Table 6.

$$P = \frac{1}{1 + e^{(6.929 - 0.867 * Age + 1.796 * Hd - 1.067 * ST - 2.177 * Sd - 1.625 * no)}} \quad (3)$$

Table 6 Classification table for shopping trip probability function

| | | Predicted | | % Correct |
|--------------------|------------------|-----------|------------------|-----------|
| | | Car | Public transport | |
| Observed | Car | 103 | 20 | 83.7 |
| | Public transport | 8 | 19 | 70.4 |
| Overall Percentage | | | | 81.3 |

proportional accuracy by chance 25% criteria = 88.1

Table 6 shows that the estimated logistic model has an overall success rate of 81.3%, which is higher than the random criteria's 25% relative accuracy of 88.1%. This suggests that the estimated logistic model does a very good job of showing between the two groups. 83.7% of respondents who used their own cars were correctly classified compared to 70.4% of respondents who used PT modes. Consequently, the 81.3% total accuracy provides information on how the model fits.

6. Validation

Table 7 summarizes the outcomes of the binary logistic model validation of the user of a shopping trip with five factors. In order to acquire the validation model, 150 test cases were introduced and subsequently chosen; the independent variables with p-values less than 0.05 served as the basis for the criteria for significant levels. With p-values less than 0.05, it seems that every factor was significant according to the p-values in this table. The likelihood that we will make a type I error, or reject the null hypothesis when it is true, is known as the significance level. Therefore, there is a 5% risk of committing a type I error if we select a significance threshold of 0.05 (strong evidence).

Table 7 Binary logistic model validation for public transport shift under shopping trip (n =150 samples)

| Variable | B | S.E. | Df | Sig. | Exp(B) | 95% C.I. for EXP(B) | |
|------------------------------|---------|-------|----|-------|---------|---------------------|----------|
| | | | | | | Lower | Upper |
| Age | -1.601 | 0.691 | 1 | 0.020 | 0.202 | 0.052 | 0.781 |
| Household size | 4.759 | 1.555 | 1 | 0.002 | 116.686 | 5.535 | 2459.763 |
| shopping travel time | -1.696 | 0.843 | 1 | 0.044 | 0.183 | 0.035 | 0.957 |
| shopping distance | -3.166 | 1.043 | 1 | 0.002 | 0.042 | 0.005 | 0.326 |
| Car ownership | -4.91 | 1.657 | 1 | 0.003 | 0.007 | 0.00 | 0.19 |
| Constant | 8.857 | 3.943 | 1 | 0.025 | 7024.85 | | |
| Summary of statistics | | | | | | | |
| -2 Log likelihood | 24.607a | | | | | | |
| Chi square | 116.811 | | 5 | 0.000 | | | |
| Cox & Snell R Square | 0.541 | | | | | | |
| Nagelkerke R Square | 0.886 | | | | | | |
| Number of observation | 150 | | | | | | |

Dependent variable: 1 = Public transport, 0 = Car

The table illustrates the significant characteristics that indicate age, household size, shopping travel time, shopping distance and car ownership with significant level 0.0000. The binomial logit model that only has two possibilities is written as in Equation 4.

$$P_a = \frac{1}{1 + e^u} \quad (4)$$

Where

- P_a = probability of own car users' switch to public transport modes
 u = utility function for bus mode
 e = the base of natural logarithms (approximately 2.718).

The study utility function for public transport is shown as in Equation 5.

$$U_b = \beta_0 + \beta_1 X_{Age} + \beta_2 X_{Hd} + \beta_3 X_{ST} + \beta_4 X_{Sd} + \beta_5 X_{no} \quad (5)$$

On the other hand, the model is

$$U_b = 8.857 - 1.601 * Age + 4.759 * Hd - 1.696 * ST - 3.166 * Sd - 4.91 * no \quad (6)$$

Where

- U_b = utility function for bus modes
 β_0 = the model specific constant
 $\beta_1, \beta_2, \dots, \beta_5$ = coefficients associated with explanatory (significant variables)
 X_1, X_2, \dots, X_5 = individual explanatory variables
Age = age
Hd = household size
ST = shopping travel time
Sd = shopping distance
no = number of own car per household.

The model's summary statistics reveal a significant correlation, indicating a perfectly fitted model, with the Nagelkerke R^2 at 0.886 (close to 1), the Cox & Snell R^2 value at 0.541 and the -2 Log likelihood (-2LL) anchored at 24.607a. According to Table 7, every variable seemed to be significant at the 0.05 level of significance. The transport switch model is still significantly impacted by age, as seen by the coefficient of -1.601 and an odds ratio of 0.202 (95% CI: 0.052-0.781). The likelihood that respondents will move to own car increase with their age, according to odds less than 1. Switching to PT is more likely when the age group decreases by one unit. A significant determinant in this switch is household size, as seen by the coefficient of 4.759 and odds ratio of 116.686 (95% CI: 5.535-2459.763). According to the positive coefficient, respondents are more likely to switch to PT for every unit increase in the household size group.

With a coefficient of 1.696 and likelihoods ratio 0.183 (95% CI: 0.035-0.957), the outcomes indicate that shopping travel time is significant factor for transport switching. Therefore, the likelihood to PT modes will decrease with an increase of own car in the shopping travel time group. Similarly, a negative coefficient of -3.166 with odds ratio 0.042 (95% CI: 0.005-0.326) are identified for the shopping distance. Therefore, people are less inclined to switch to PT the farther they have to go shopping. In particular, decreasing the shopping travel distance group by one unit will increase the probability of selecting PT modes. In the end, the number of people who own cars has a big influence on transportation switching. According to a likelihood ratio of 0.007 (95% CI: 0-0.19) and a Coefficient of -4.91, respondents who own car are less likely than those who do not to use PT. it is easy to see that the likelihood of using PT option reduces with every unit increase in the number of own car users. The outcomes of the binary logistic regression with (750) data points are consistent with the evaluation of the coefficient, which clearly shows that independent variables like age, shopping travel time, shopping distance, and own car ownership are significant and have negative value. However, the independent variable, such as household size is shown to be significant, which is in line with the outcome of the current data. A positive coefficient indicates that the likelihood of switching to PT modes increases with household size. As demonstrated in table 8, the classification table also assesses the model's validation. The estimated logistic model's overall success rate of 96% was higher than the proportional accuracy of 25% and the criteria of 88.1% by chance, indicating that the estimated logistic model effectively distinguishes between the two groups. 88.9% of respondents who used PT were properly predicted compared to 97.6% of respondents who used their own cars. As an outcome, the 96% overall accuracy indicates that the model fits the data well.

Table 8 Classification table for model validation under shopping trip (n=150 samples)

| | | Predicted | | |
|--------------------|------------------|-----------|------------------|-----------|
| | | Car | Public transport | % Correct |
| Observed | Car | 120 | 3 | 97.6 |
| | Public transport | 3 | 24 | 88.9 |
| Overall Percentage | | | | 96.0 |

proportional accuracy by chance 25% criteria = 88.1

7. Conclusion

This research examines the behaviour of transport users in Tripoli roads between two current transport modes available, namely private transport vehicles as (own car, taxi, minibuses) and public transportation vehicles, and it determines the switch to that travellers make when choosing their transport mode. As the mode switch model between using PT and driving own car. To investigate the factors influencing PT users and predict the likelihood of a change in PT users with regard to different shopping travel times and distances, a binary logistic model



for shopping trip was created for two options; own car and PT modes. In order to ascertain the relative influence of demographic and socio-economic and mode attributes on the mode switch behaviour, the model looks at the features of both owning a car and using PT, including shopping travel time, shopping travel distance and characteristics to determine the relative influence of demographic, socio-economic characteristics. In actuality, every variable was significant at 0.05 level. A wide range of respondent's viewpoints and their likelihood of selecting the best travel services are indicated by the probability prediction of policy switch. Nurdden et al. have identified the factors that prevent private car users from using public transport so that rational policies could be express to encourage greater use of public transport [11]. Mackett have identifies different policy actions to reduce own car use for different types of trips as shopping trip and the actions that are required to meet the travel needs that the car currently fulfils [12]. Reduced shopping travel time and the availability of dedicated lanes for PT modes were the two most significant factors that were determined to be likely to encourage the usage of PT. **Finally**, it has been concluded that the factors playing a significant role in the switch own cars ownership to public transportation modes include reducing shopping travel time. By improving this factor through the introduction of public transport services into the road network of Tripoli, a large proportion of respondents from residential area in Tripoli will switch to the public transport, which will also contribute to enhancing environmental protection and ecological balance. Accordingly. In order to optimize travel time for all types of city trips, this study suggests a few measures to promote the use of the public transportation system with divided lanes on Tripoli's network roadways.

References:

- [1] Amiruddin, ISMAI & Adel Elmloshi 2011, Travel Time is the Main Factor for Switching Travel Mode in Tripoli Street: Proceedings of the Eastern Asia Society for Transportation Studies, Vol.8, 2011
- [2] Regional workshop on urban transport in the Mediterranean Region, Blaikie 2003, Janury 22&23,2008 – Skhirat- Morocco.
- [3] Adel Elmloshi. 2019. Probability of policy shift to public transport. Case study: Tripoli – Libya. International Conference on Technical Sciences (ICST2019) March 2019 04 – 06
- [4] Alrabotti, F. B.2007. *Traffic Lights, part two – (Tripoli)*, General people's committee of general secretariat (ministry) of Libya justice and directorate general of traffic and licensing.
- [5] Schrank, D. L. & Lomax T. J. 1997. Traffic congestion; transportation; urban transportation policy; traffic flow; planning; United States, Texas Transportation Institute, Texas A & M University System (College Station, Tex. and Springfield, Va.), 100-385-610 (*Last edited on 27 Feb US/Mountain*).
- [6] Amiruddin Ismail, Adel Elmloshi 2011. Introducing Public Transport System to Improve Travel Time and Road Safety in Tripoli, Libya. Australian Journal of Basic and Applied Sciences, 5(6): 563-569, 2011 ISSN 1991-8178
- [7] Abuhamoud M. A. 2012. Modelling modal shift and parking management in Tripoli City centre - (libya). Thesis Submitted In Fulfilment For The Degree of Doctor of Philosphy. Faculty of Engineering and Built Enveronment, Universiti Kebangsaan Malaysia, Bangi.
- [8] Bajracharya A. R., 2008. The impact of modal shift on the transport ecological foot print, A case study of the proposed Bus Rapid Transit System in Ahmedabad, India, thesis submitted to the International Institute for Geo-information Science and Earth Observation in partial fulfilment of the requirement for the degree of



Gharyan University Journal of Engineering Science (GUJES)

Website: <http://gujes.gu.edu.ly>

email: gujes@gu.edu.ly



Master of Science in Geo-information Science and Earth Observation, Specialisation: Urban Planning Management. Enscheda, the Netherlands.

- [9] Dayton, C. M. 1992. Logistic regression analysis, department of measurement, statistics & evaluation, room 1230d benjamin building, University of Maryland.
[http://bus.utk.edu/stat/datamining/Logistic%20Regression%20Analysis%20\(Dayton\).pdf](http://bus.utk.edu/stat/datamining/Logistic%20Regression%20Analysis%20(Dayton).pdf) [28 Oct 2013].
- [10] Essia Taleb Essia Ali 2009. Why do post graduate students use private cars, dissertation submitted in Partial Fulfilment of the Requirements for the Degree of Master of Engineering. Faculty of Engineering and Built Environment. Universiti Kebangsaan Malaysia, Bangi.
- [11] Nurdden Abdullah, Riza Atiq O.K. Rahmat, & Amirudden Ismail. 2007. Effect of Transportation Policies on Model Shift from Private Car to Public Transport in Malaysia. *Journal of Applied Sciences* 7 (7): 1013-1018.
- [12] Mackett, R.L. 2003. Why do people use their cars for short trips? *Transportation Journal* 30: 329-349.



Comparative Analysis of Soil Resistivity Measurements Using Wenner Four-Point Method: A Case Study in Sabratha, Libya

S. Mousa^{1*}, I. Abood², A. Essed³, M. Alhawwari⁴, M. Almaysawi⁵

¹Electrical and Electronic Department, Sabratha University, Sabratha, Libya, Salah.Mousa@Sabu.edu.ly

²Electrical and Electronic Department, University of Gharian, Gharian, Liby, aboodali1966@gmail.com

³Electrical and Electronic Department, Sabratha University, Sabratha, Libya, abdulhamed.essed@Sabu.edu.ly

⁴Electrical and Electronic Department, Sabratha University, Sabratha, Libya, Misbah.Alhawwari@Sabu.edu.ly

⁵Electrical and Electronic, Libyan Academy, Janzour, Libya, Mohamed.Misway@gmail.com

*Corresponding author: Salah.Mousa@Sabu.edu.ly

Abstract

Accurate soil resistivity measurements are essential for the effective design of grounding systems, particularly in environments where soil properties vary significantly with depth and environmental conditions. This study presents a comparative analysis of soil resistivity measurements using the Wenner four-point method at two test sites in Sabratha, Libya. Measurements were conducted using both Megger and Fluke instruments to evaluate data consistency and identify subsurface variability. Results show that while shallow-depth readings were consistent across devices, significant divergences occurred at greater depths due to heterogeneous soil layering. The analysis reveals a distinct variation in resistivity profiles across different locations and instruments, indicating layered soil structures and fluctuating conductivity due to environmental factors such as rainfall. Results from the Megger and Fluke instruments show consistency at shallow depths but diverge at greater depths, with Fluke detecting a steeper drop in resistivity, potentially signifying a deeper transition to more conductive layers. three-layer soil model derived through CDEGS simulation further validated field observations, indicating a highly resistive intermediate layer overlying a more conductive sublayer. These findings underscore the importance of multi-depth profiling and instrument selection in designing robust and safe earthing systems.

Keywords: Soil Resistivity, Earthing Systems, Wenner Method, Instrumentation Comparison, Sodium Chloride, Bentonite

1. Introduction

Soil resistivity is a key factor that affects how well grounding systems perform. Therefore, accurate soil resistivity measurements and modeling are essential for predicting the behavior of grounding systems in such high soil resistivity [1]. Soil Resistivity significantly depends on soil composition, moisture content, temperature, and other environmental factors [2]. A high soil resistivity can lead to inadequate grounding, which poses safety risks and may cause equipment malfunction. Therefore, understanding and properly assessing soil resistivity helps engineers design grounding systems that are both safe and efficient, ensuring that electrical faults are properly dissipated into the earth. The primary goal of grounding is to provide a safe path for discharging excess currents resulting from electrical faults or lightning strikes, thereby protecting individuals from the risk of electric shock and safeguarding equipment. Grounding theory is based on physical principles such as equalizing electrical potentials between different



metallic parts, preventing dangerous voltage differences. Various configurations have been devised for measuring soil resistivity, with the Wenner method illustrated in [3]—being one of the most commonly used techniques. Although it is not typically recommended for power engineering applications [2], soil resistivity can still be assessed in laboratory settings using alternative methods [4].

The motivation for this paper stems from the growing need to design efficient and reliable grounding systems in high soil resistivity sites.

2. Factors Affecting Soil Resistivity

Soil resistivity is a variable characteristic that indicates how much the soil resists the flow of electrical current. It is influenced by a variety of physical, chemical, and environmental factors, making it a critical parameter in fields such as electrical engineering, geotechnical studies, and agriculture. Understanding these factors is essential for designing effective grounding systems, preventing corrosion, and optimizing agricultural practices. Below is an explanation of the key factors affecting soil resistivity:

2.1 Soil Type

The type of soil plays a significant role in determining its resistivity. Soil is composed of various minerals and organic materials, and its resistivity varies depending on its composition. For example, clayey soil contains minerals like montmorillonite or kaolinite, which have a high surface area and can retain water and ions, making it highly conductive and resulting in low resistivity (10–100 $\Omega\cdot\text{m}$) [5].

2.2 Moisture Content

Moisture is one of the most critical factors affecting soil resistivity. Water acts as a conductor when it contains dissolved ions, such as calcium (Ca) or magnesium (Mg). As the moisture content in the soil increases, its resistivity decreases significantly [5].

2.3 Salt Content

The type of salt also influences resistivity; highly soluble salts like sodium chloride have a more pronounced effect compared to low-solubility salts like calcium sulfate. In coastal areas or regions with saline groundwater, soil resistivity is typically very low due to the high salt content [5].

2.4 Temperature

Temperature has a direct impact on soil resistivity. At low temperatures (below 0°C), water in the soil freezes, stopping the movement of ions and sharply increasing resistivity. Conversely,

at higher temperatures (25–50°C), ion movement increases, reducing resistivity. However, if high temperatures lead to evaporation and drying of the soil, resistivity may increase again due to the loss of moisture [5].

2.5 Soil Stratification

Soil is often composed of multiple layers, each with different properties. For example, a clayey surface layer with low resistivity may overlie a rocky layer with high resistivity. This stratification affects the overall resistivity of the soil and must be considered when designing systems like grounding networks [5].

2.6 Chemical Contamination

Chemical pollutants can alter the resistivity of soil. For example, acids like sulfuric acid can dissolve minerals and increase the concentration of ions, reducing resistivity. On the other hand, oils or petroleum can form an insulating layer on soil particles, increasing resistivity [5].

3. Wenner Four Point Method

Methods for measuring soil resistivity include using an Earth Resistance Meter, which operates based on the four-electrode method. This involves inserting four metal electrodes into the soil and connecting them to the device to measure resistivity. Methods for measuring soil resistivity include using an Earth Resistance Meter, which operates based on the four-electrode method. This involves inserting four metal electrodes into the soil and connecting them to the device to measure resistivity.

Measuring soil resistivity is fundamental in the case of designing an earthing system. The factors that affect soil resistivity have been explored, therefore, by establishing an accurate way of measuring soil resistivity, models can be produced to generate valid simulations and contribute to a good earthing design. Comprehensive studies have been conducted to establish a soil resistivity measurement technique with the main method being the Wenner method [6]. This measurement involves a four-probe array in a straight line that is inserted into the earth of equal depth with a spacing that is constant. The two outer probes are used to inject a test current and the two inner probes are used to measure the potential difference across the two points. A simple rearrangement using Ohm's law gives the resistance of the soil. Figure 1 shows a model of the Wenner arrangement.

It was deduced by Wenner [6,7] that the soil resistivity can be determined by using Equation 1.

$$\rho = 2\pi aR \quad (1)$$

Where:

a: is the distance between the probes (m)

R: is the measured resistance (Ω)

ρ : is the calculated soil resistivity ($\Omega.m$)

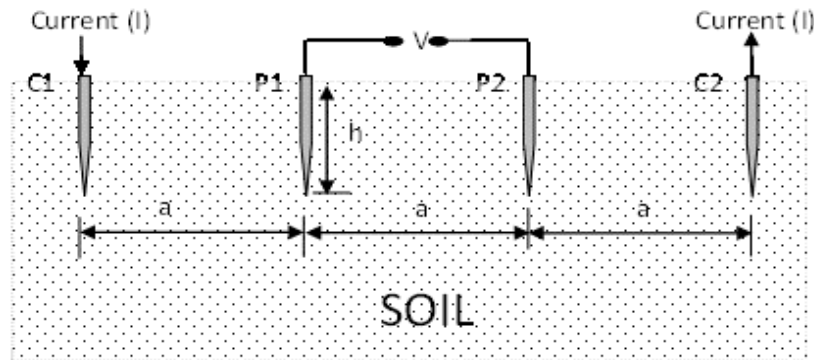


Figure 1: Wenner Four Probe Method [6]

4. Result and Discussion

The test site used to conduct all measurements was on a farm at Sabratha city (Talil). Figure 2 shows an aerial view of the farm detailing the locations of the test sites. The Wenner method was used to measure the soil resistivity for both sites a and b. Two profile tests were performed, and the profile one is perpendicular to profile two and both were measured at the same time and has the same length (39m).



Figure2: Satellite image of measurement location at Sabratha test site

The Megger DET4TR2 was used, and it is an advanced device for measuring earth resistance and features several characteristics that make it suitable for use in various environments. Figure 3 compares the soil resistivity measurements for two distinct profiles. The graph illustrates how soil resistivity ($\Omega \cdot m$) varies with Wenner spacing (in meters), indicating the subsurface soil properties at increasing depths. Both profiles show initial increases in resistivity, suggesting a

near-surface resistive layer (e.g., dry or rocky soil). Profile one exhibits higher resistivity and a broader peak compared to profile two, possibly indicating a thicker or more resistive upper layer. The decrease in resistivity for both profiles at greater spacings implies the presence of a deeper, more conductive layer (e.g., moist or clayey soil). However, the resistivity in profile two decreases more rapidly than in profile one, which could suggest a thinner resistive layer or a shallower transition to a conductive layer.

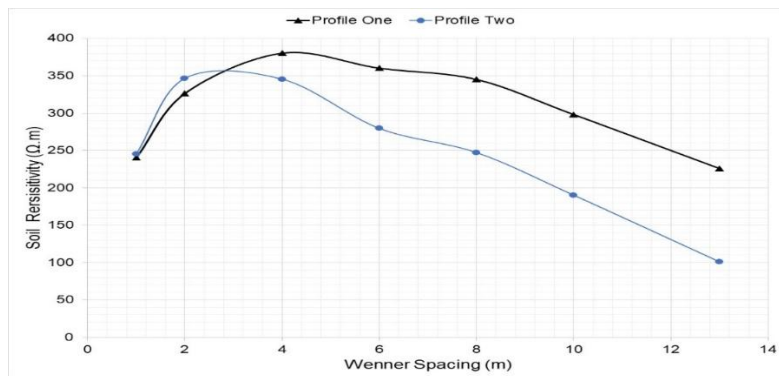


Figure 3: soil resistivity measured by Megger

Figure 4 presents a graph comparing soil resistivity values at Site a and Site b as a function of Wenner Spacing (measured in meters). At Site a, resistivity initially shows an increasing trend, followed by a decline. This pattern suggests the presence of a resistive layer (e.g., dry or rocky material) beneath the surface, which is more pronounced at intermediate spacings. As the spacing increases, the resistivity starts to decrease, possibly indicating a transition to a more conductive layer, such as moist or clayey soil.

In contrast, Site b exhibits a steady decline in resistivity with increasing spacing. This consistent decrease suggests an increase in soil conductivity, likely due to higher moisture content or the presence of clayey materials.

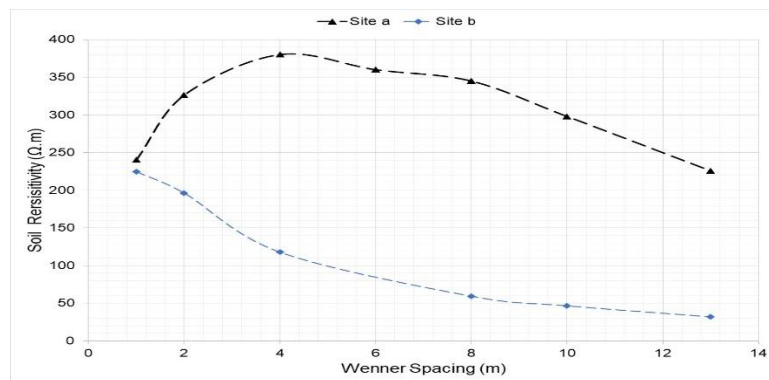


Figure 4: Variation of Soil Resistivity with Wenner Spacing at Different Sites

Figure 5 shows a comparison of soil resistivity measurements taken using two different instruments: Megger and Fluke, across various Wenner Spacing values (in meters). Wenner spacing (a) represents the spacing between electrodes in the Wenner method of soil resistivity testing. Greater spacing allows measurements deeper into the ground. As can be seen from figure that both instruments start with very similar readings at smaller spacings (1–2 m), indicating consistency at shallow depths. At the middle-range spacing (4–8m), the readings show some deviation. Fluke instrument shows a small peak at 6m and its values tend to be higher than Megger instrument, while Megger shows a smoother curve. At the large spacing (14m), Fluke shows a much sharper drop compared to Megger, suggesting it detects a significant change in soil composition or moisture content deeper down.

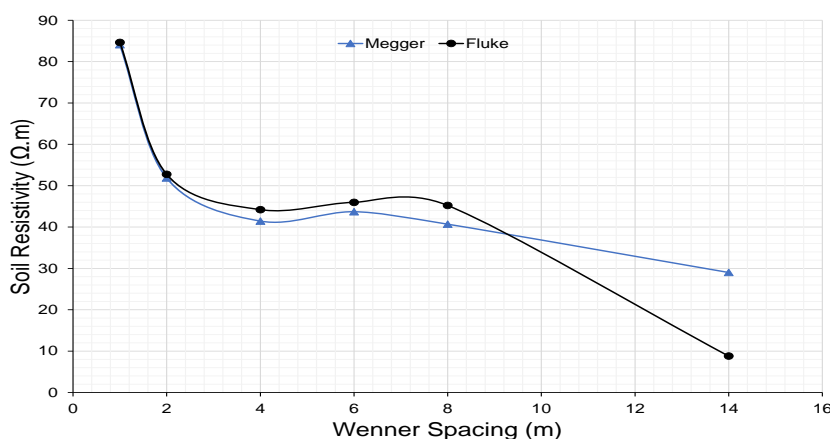


Figure 5: Comparison of Soil Resistivity Measurements Using Megger and Fluke Instruments at Varying Wenner Spacings

4.1 Soil Treatment

To reduce the earthing (grounding) resistance for any type of earth electrode, the low soil resistivity and high conductivity materials are usually used. In the past, the Chloride Sodium was often used, but this type of the salt has some disadvantages such as causing a corrosion for the material of the vertical electrode. Today, a lot of materials were used such as the Bentonite (Clay) which has low resistivity and retain moisture, which can help to increase the conductivity. In this paper, the comparison between the Chloride Sodium and bentonite was performed at the field to reduce the earthing resistance of the vertical electrode, as shown in Figure 6. In this test, a 1m vertical electrode was used, and 3inches of the Chloride Sodium and Bentonite layers are being used surrounding the vertical electrode.

The results were tabulated in table 1. as can be seen from the table that, using the Sodium Chloride dropped the resistance significantly to 44.10 Ω , resulting in an 85.2% reduction. However, Bentonite reduced the resistance to 58.70 Ω , which is also a strong improvement,

with an 80.3% reduction which slightly less effective than NaCl, it is beneficial in environments where long-term moisture retention is needed.

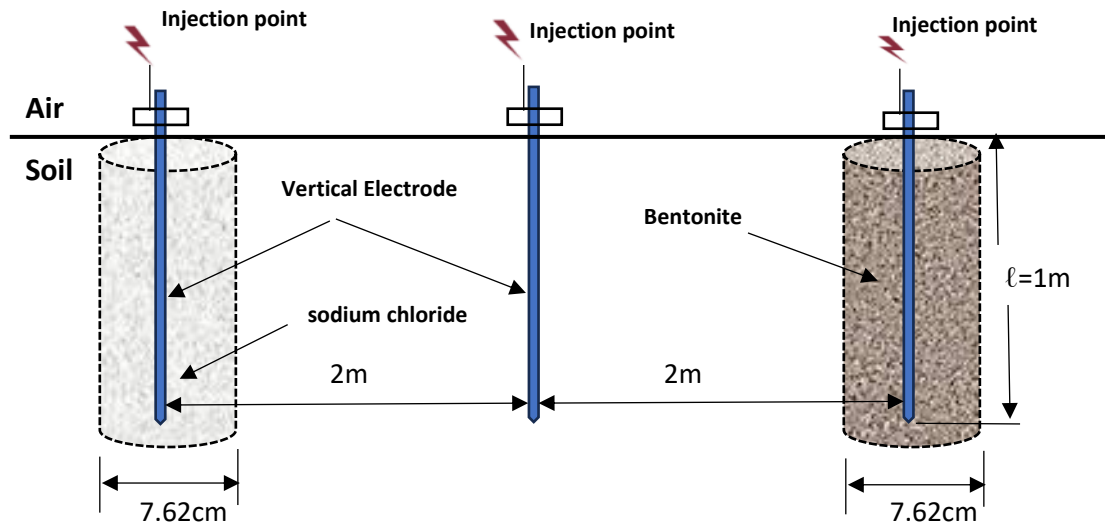


Figure 6: Experimental Setup for Treated Vertical Earthing Electrode in Soil

The results were tabulated in table 1. as can be seen from the table that, using the Sodium Chloride dropped the resistance significantly to 44.10 Ω , resulting in an 85.2% reduction. However, Bentonite reduced the resistance to 58.70 Ω , which is also a strong improvement, with an 80.3% reduction which slightly less effective than NaCl, it is beneficial in environments where long-term moisture retention is needed.

Table1 Impact of Sodium Chloride and Bentonite on Earthing Electrode Performance

| Configuration | Earthing Resistance (Ω) | Reduction Percentage (%) |
|--------------------------------|----------------------------------|--------------------------|
| Rod only | 298.00 | ----- |
| Rod with 3inch Sodium Chloride | 44.10 | 85.20 |
| Rod with 3inch Bentonite | 58.70 | 80.30 |

4.2 Soil Resistivity Simulation

The soil for the resistivity simulation using CDEGDS software (Current Distribution Electromagnetic Grounding Systems) [8] at test site will be used throughout. Table 2 shows the most recently derived soil model. As can be seen from the from the table, it's clear that there are three-layer soil model. The top soil resistivity layer is 196.35 Ω .m with 1.19 m Depth. This represents the uppermost soil layer, often closest to the surface. It could indicate moderately resistive soil, such as dry topsoil or compacted ground. The second layer is the

Middle Layer, and the value of soil Resistivity is 2107.62 $\Omega \cdot m$ with depth 0.92m. A highly resistive layer, possibly representing a rocky or very dry layer with minimal moisture content. The third layer is called lower layer, and its value is 55.68 $\Omega \cdot m$. A conductive layer likely consisting of moist soil, clay, or water-saturated materials, commonly found deeper underground.

Table2 Soil Resistivity Simulation using CDEGS Software

| 3 Layer Model | Top | | Middle | | Lower | |
|---------------|----------------------------|-----------|----------------------------|-----------|----------------------------|-----------|
| | Resistivity (Ωm) | Depth (m) | Resistivity (Ωm) | Depth (m) | Resistivity (Ωm) | Depth (m) |
| | 196.35 | 1.19 | 2107.62 | 0.92 | 55.68 | ∞ |
| Uniform Model | Resistivity (Ωm) | | | | | |
| | 196.35 | | | | | |

5. Conclusion

Soil resistivity, a key property that determines the soil's ability to conduct electrical current, is influenced by a multitude of factors, including soil type, moisture content, temperature, salt content, density, and chemical composition. Understanding these factors is essential for designing effective grounding systems, especially in constrained sites where soil conditions may pose significant challenges.

This study underscores the significance of accurate soil resistivity measurements for the design of reliable grounding systems. By employing the Wenner four-point method and comparing results from the Megger and Fluke instruments, the research identified layered soil structures and the impact of environmental factors such as moisture and rainfall on resistivity profiles. The findings revealed consistent measurements at shallow depths but notable divergences at greater depths, with the Fluke instrument indicating a sharper transition to conductive layers. These variations highlight the necessity of multi-depth analysis and careful instrument selection to account for subsurface heterogeneity. The results provide valuable insights for engineers designing grounding systems in complex soil environments, ensuring safety and operational efficiency. Finally, the findings highlight the necessity of employing multi-depth resistivity profiles and cross-instrument comparisons in order to obtain a comprehensive understanding of the soil structure. Such insights are pivotal for the engineering of reliable and effective grounding systems, especially in high-resistivity or environmentally dynamic regions. Future work could explore seasonal effects and expand testing across diverse soil types to develop adaptable grounding models. Finally, the results show that excellent effectiveness for NaCl's better than Bentonite due to ability to attract moisture and improve ion mobility in the soil.



References

- [1] O. Kherif, S. Robson, N. Harid, D. Thorpe, S. Stivanello and A. Haddad, "On the Impact of Soil Resistivity Measurement and Modelling on Grounding Performance," 36th International Conference on Lightning Protection (ICLP), Cape Town, South Africa, pp. 379-382, 2022
- [2] O. Kherif, S. Robson, N. Harid, D. Thorpe, S. Mousa, S. Stivanello and A. Haddad, "Impact of Profile Orientation and Position on Soil Resistivity Measurement for Earthing Applications," 58th International Universities Power Engineering Conference (UPEC), Dublin, Ireland, ,Page(s):1 – 5, 2023.
- [3] O. Kherif, S. Robson, S. Mousa, N. Harid, H. Griffiths, D. Thorpe, A. Haddad, "Toward Enhancing Soil Resistivity Measurement and Modelling for Limited Interelectrode Spacing", IEEE Transactions on Electromagnetic Compatibility, vol.67, no.2, pp.374-383, 2025.
- [4] Standard Test Method for Measurement of Soil Resistivity Using the Wenner Four-Electrode Method", ASTM International, West Con shohocken, PA, USA, ASTM G57-20.
- [5] BS Standrad 7430,"Code of practice for protective earthing of electrical installations", 2011
- [6] F. Wenner, "A method for measuring earth resistivity," Bureau of Standards Scientific Paper, no. 258, 1915
- [7] IEEE Standard 81,"Guide for Measuring Earth Resistivity, Ground Impedance, and Earth Surface Potentials of a Grounding System", 2012
- [8] SES (Safe engineering services). Current distribution electromagnetic grounding analysis software (CDEGS), <http://www.sestech.com/products/softpackages/cdegs.htm>

أثر إدارة سلسلة التوريد وعلاقتها بأداء الشركات الصناعية (دراسة ميدانية على إحدى الشركات المصنعة بالسوق الليبي)

محمد البهلول أحمد البكاي¹، نورالدين التومي²، اسيل عادل جالوته³

¹ جامعة غريان، غريان، ليبيا، ElBakai1989@gmail.com

² جامعة غريان، غريان، ليبيا، aan.toumi@gmail.com

³ مركز البحوث النفط طرابلس، طرابلس، ليبيا، Jaulta@gmail.com

*Corresponding author: elbakai1989@gmail.com

الملخص

تسعي الدراسة إلى تحقيق مجموعة من الأهداف، أبرزها تحديد تأثير ممارسات إدارة سلسلة التوريد على تحسين أداء إحدى الشركات الوطنية. حيث تركز الدراسة على الدور الرئيسي لعدة عوامل، منها العلاقة مع الموردين، العمليات الداخلية، العلاقة مع الوسطاء، العلاقة مع العملاء، ومشاركة المعلومات في تعزيز كفاءة الشركة. بالإضافة إلى ذلك، و من أجل تحسين أداء الشركة سعت الدراسة إلى تسليط الضوء على أهم الممارسات التي تساهم بشكل كبير بواقع تطبيق تلك الممارسات. ولذلك فإن هذه الدراسة تبين بالتفصيل إمكانية تطبيق ممارسات إدارة سلاسل التوريد الخاصة بشركة النسيم للصناعات الغذائية، و أثر ذلك على أداء سير و سرعة الاستجابة للعمليات. اتبعت الدراسة المنهج الوصفي والاستدلالي، معتمدةً على أسلوب التحليل في استعراض الإطار النظري والدراسات السابقة ذات العلاقة. واستخدمت استبانة كأداة رئيسية لجمع البيانات من عينة الدراسة المكونة من (15) مختصاً في إدارة سلسلة التوريد بشركة النسيم للصناعات الغذائية. وقد تم تحليل البيانات باستخدام برنامج SPSS عبر مجموعة من الأساليب الإحصائية، مثل التكرارات، النسب المئوية، المتوسطات، واختبارات الصدق والثبات، التوزيع الطبيعي بالإضافة إلى الارتباط والانحدار البسيط. أظهرت نتائج الدراسة وجود تطبيق واسع لأبعاد ممارسات إدارة سلسلة التوريد بنسبة (69.6%)، حيث جاء في المرتبة الأولى بُعد العمليات الداخلية بنسبة، تلاه بُعد العلاقة مع العملاء و الموردين، ثم بُعد مشاركة المعلومات علي التوالي بينما احتلت العلاقة مع الوسطاء المرتبة الأخيرة بنسبة لم تتجاوز. كما أكدت النتائج أن لهذه الممارسات دوراً كبيراً في تحسين الأداء التشغيلي للشركة، حيث إن نسبة كبيرة من التغيير في الأداء تعزى إلى تطبيق ممارسات إدارة سلسلة التوريد. وفي ضوء النتائج، أوصت الدراسة بضرورة تعزيز اهتمام الشركة بتطبيق ممارسات إدارة سلسلة التوريد، خاصة فيما يتعلق بالعلاقة مع الوسطاء ومشاركة المعلومات، نظراً لانخفاض مستوى التركيز عليهما نسبياً. علاوة على ذلك، أوصت الدراسة بتطوير بعض الممارسات الداخلية ضمن كل بُعد لتعزيز الكفاءة و الرفع من مرونة سلسلة التوريد والتعاون والتكامل في شبكتها.

الكلمات المفتاحية: إدارة سلسلة التوريد، أداء الشركات الصناعية، سوق ليبيا، العمليات التشغيلية.

1. المقدمة

تعد إدارة سلسلة التوريد (Supply Chain Management – SCM) من المفاهيم الإدارية الحديثة التي تسهم بشكل مباشر في تحسين كفاءة الشركات وزيادة قدرتها التنافسية، حيث أصبحت من العوامل الرئيسية التي تؤثر على نجاح واستدامة الشركات في مختلف القطاعات الصناعية والتجارية. وتُعرف إدارة سلسلة التوريد بأنها التنسيق الفعال للأنشطة اللوجستية والإنتاجية والتوزيعية داخل المنظومة التجارية، بدءاً من توريد المواد الخام، مروراً بعمليات التصنيع، وانتهاءً بوصول المنتجات

إلى المستهلك النهائي [1]. وتعتمد الإدارة الفعالة لسلسلة التوريد على مجموعة من الاستراتيجيات والتقنيات الحديثة التي تهدف إلى تحسين الكفاءة التشغيلية، تقليل التكاليف وتعزيز مستوى رضا العملاء [2]. كما أن الشركات التي تطبق استراتيجيات فعالة في إدارة سلاسل التوريد تتمتع بميزة تنافسية واضحة من خلال تحقيق مرونة أكبر في التعامل مع التغيرات في الأسواق وتحسين سرعة الاستجابة لاحتياجات العملاء [3]. وتشير الدراسات إلى أن الشركات التي تتبنى نهجاً متكاملاً في إدارة سلاسل التوريد تحقق مكاسب تنافسية واضحة مقارنةً بتلك التي لا تطبق استراتيجيات فعالة في هذا المجال [4]. رغم الفوائد العديدة التي تحققها إدارة سلسلة التوريد، إلا أن هناك العديد من التحديات التي قد تعيق تحقيق الأداء الأمثل، ومنها عدم الاستقرار الاقتصادي، والتغيرات في الطلب، والمشاكل اللوجستية، وعدم كفاءة الموردين [5] في الأسواق الناشئة مثل السوق الليبي، حيث تواجه الشركات الصناعية تحديات إضافية مثل عدم استقرار سلاسل التوريد، ضعف البنية التحتية اللوجستية، والاعتماد على الاستيراد في توفير المواد الخام مما يجعل من الضروري تبني استراتيجيات مرنة وقابلة للتكيف مع هذه الظروف [6].

2. منهجية البحث

نظراً لطبيعة هذه الدراسة والأهداف التي تسعى إلى تحقيقها، والتي تركز على أثر ممارسات إدارة سلسلة التوريد في تحسين أداء الشركات الصناعية، فقد اعتمد البحث على كل من المنهج الوصفي والمنهج التحليلي. حيث تم توظيف المنهج الوصفي في استعراض المفاهيم النظرية ذات الصلة، في حين تم تطبيق المنهج التحليلي في معالجة البيانات المستخلصة من الاستبيان الموزع كجزء من الدراسة التحليلية التطبيقية.

تم تطوير استبانة بعد الرجوع إلى الأدب النظري والدراسات السابقة ذات الصلة بموضوع البحث، حيث تمت الاستفادة من الاستبانات المستخدمة في الدراسات السابقة مع إجراء تعديلات تتناسب مع أهداف الدراسة. وقد صيغت مجموعة من الفقرات تم درجها ضمن تسعة أبعاد رئيسية مما يسهم في تحقيق تحليل دقيق لموضوع البحث. يتمثل مجتمع الدراسة في الفئة المختصة بإدارة سلسلة التوريد ضمن أقسام التخطيط، المشتريات، المخازن، الإنتاج والجودة بشركة النسيم للصناعات الغذائية. وبما أن حجم المجتمع محدود، تم استخدام أسلوب الحصر الشامل حيث تم توزيع 15 استبانة على مجتمع الدراسة. بعد استكمال جمع البيانات، تم تحليلها ودراسة العلاقات بين متغيرات البحث الرئيسية كما هو مبين بالجدول (1) لاختبار الفرضيات المطروحة باستخدام البرنامج الإحصائي للعلوم الاجتماعية (Statistical Package For Social Science - SPSS) والذي ساهم في استخلاص النتائج وصياغة التوصيات التي يمكن أن تسهم في تطوير أداء الشركات الصناعية من خلال تحسين ممارسات إدارة سلسلة التوريد.

جدول (1) يوضح ابعاد وفقرات أداة الدراسة

| عدد الفقرات | الابعاد | المتغيرات الرئيسية |
|-------------|-----------------------|--|
| 5 | العلاقة مع الموردين | المتغير المستقل ممارسات ادارة سلسلة التوريد |
| 6 | العلاقات الداخلية | |
| 5 | العلاقة مع الوسطاء | |
| 5 | العلاقة مع العملاء | |
| 8 | المشاركة في المعلومات | |
| 29 | اجمالي الفقرات | |
| 4 | التكلفة | المتغير التابع تحسين اداء الشركة |
| 3 | الجودة | |
| 4 | المرونة | |
| 2 | التسليم | |
| 13 | اجمالي الفقرات | |

3. تحليل وعرض النتائج

3.1 اختبار الفرضية الرئيسية الاولى

تنص هذه الفرضية علي: "لا يوجد تطبيق بدرجة مناسبة وذو دلالة احصائية عند مستوى معنوية (0.05) لممارسات إدارة سلسلة التوريد في الشركة" و تهدف هذه الفرضية الى معرفة واقع تطبيق ممارسات ادارة سلسلة التوريد في الشركة بشكل عام. توضح البيانات المدرجة بالجدول (2) ان المتوسط العام للمتوسطات الحسابية لممارسات إدارة سلسلة التوريد في شركة النسيم بلغ (3.48)، الوزن النسبي (69.6%)، قيمة اختبار T يساوي (20.19) و مستوى الدلالة المعنوية (Sig.) تساوي (0.000) أي اقل من قيمة مستوى الدلالة المعتمد. و عليه هذا يعني رفض الفرض العدمي و قبول الفرض البديل أي ان هناك تطبيقاً بدرجة مناسبة لممارسات إدارة سلسلة التوريد بمستوى كبير.

جدول (2) المتوسطات الحسابية و الوزن النسبي لمحور ممارسات ادارة سلسلة التوريد

| م | البعد | المتوسط الحسابي | الانحراف المعياري | الوزن النسبي | قيمة T | مستوى الدلالة | الترتيب |
|---|-----------------------|-----------------|-------------------|--------------|---------|---------------|---------|
| 1 | العلاقة مع الموردين | 3.59 | 0.6 | 71.8% | 23.171 | 0.000* | 2 |
| 2 | العمليات الداخلية | 3.53 | 0.619 | 70.6% | 22.104 | 0.000* | 3 |
| 3 | العلاقة مع الوسطاء | 3.07 | 0.608 | 61.4% | 19.538 | 0.000* | 5 |
| 4 | العلاقة مع العملاء | 3.83 | 0.8 | 76.6% | 18.537 | 0.000* | 1 |
| 5 | المشاركة في المعلومات | 3.38 | 0.743 | 67.6% | 17.604 | 0.000* | 4 |
| | المتوسط العام | 3.48 | 0.674 | 69.6% | 20.1908 | 0.000* | |

*دالة احصائية عند مستوي (0.05)

3.2 اختبار الفرضية الرئيسية الثانية

تنص هذه الفرضية على : " لا دور ذو دلالة إحصائية عند مستوى معنوية (0.05) لممارسات إدارة سلسلة التوريد بالشركة ". حيث تهدف هذه الفرضية إلى معرفة دور ممارسات إدارة سلسلة التوريد في تحسين أداء الشركة في حين ينبثق من هذه الفرضية خمس فرضيات فرعية أخرى كما هو موضح في 4.2.1. تشير بيانات الجدول (3) إلى أن قيمة معامل الارتباط (R) بلغت حوالي (0.79) و هي قيمة تدل على وجود ارتباط موجب قوي ذو دلالة إحصائية بين أبعاد ممارسات إدارة سلسلة التوريد إجمالاً كمتغير مستقل و تحسين الأداء كمتغير تابع. كما تشير قيمة معامل التحديد (R-Square) إلى أن ما نسبته (62.4%) من التغير الحاصل في تحسين الأداء يُعزى للتغير في أبعاد ممارسات إدارة سلسلة التوريد أما القيمة المتبقية (37.6%) من المئة تعود إلى عوامل أخرى و ما يؤكد صحة العلاقة قيمة اختبار (F) الذي يشير إلى صلاحية النموذج و معنوية هذه النتائج عند مستوى دلالة أقل من (0.05). و تظهر نتائج التحليل الإحصائي لاختبار الفرضية الرئيسية الثانية أن قيمة (B) كانت (0.79) مما يعني أن ممارسات إدارة سلسلة التوريد لها دور في تحسين الأداء و بنسبة (79%) إذا تغيرت (α) بمقدار وحدة واحدة. و بناءً على النتائج السابقة و مستوى المعنوية البالغ (0.000) فقد أسفر اختبار هذه الفرضية عن رفض الفرضية العدمية، و قبول الفرضية البديلة و التي تنص على أنه يوجد دور ذو دلالة إحصائية عند مستوى معنوية (0.05) لممارسات إدارة سلسلة التوريد في تحسين أداء شركة النسيم للصناعات الغذائية.

دول رقم (3) نتائج علاقة ممارسات إدارة سلسلة التوريد في تحسين الأداء

| المتغير المستقل | معامل الارتباط R | معامل التحديد R-Square | قيمة F | الدلالة Sig | قيمة B | قيمة T | الدلالة Sig | VIF |
|-----------------------------|------------------|------------------------|--------|-------------|--------|--------|-------------|-------|
| ممارسات ادارة سلسلة التوريد | 0.790 | 0.624 | 21.560 | 0.000 | 0.790 | 4.643 | 0.000 | 1.000 |

*دالة إحصائية عند مستوي (0.05).

3.2.1 اختبار الفرضيات الفرعية من الفرضية الرئيسية الثانية:

يبين الجدول (4) نتائج اختبار الفرضيات الفرعية من الفرضية الرئيسية الثانية حيث أظهرت قيمة معامل الارتباط (R) ما نسبته (0.52-0.708) و هذا مؤشر لوجود ارتباط موجب و ذو دلالة إحصائية بين كل بعد كمتغير مستقل و كمتغير تابع في تحسين الأداء. أما المتغير الحاصل في الأداء و الذي يشار إليه بقيمة معامل (R-Square) فقد سجل ما نسبته (43.1% - 60.9%) يُعزى هذا لإبعاد ممارسات إدارة سلسلة التوريد و النسبة المتبقية تعود إلى متغيرات أخرى و ما يؤكد صحة العلاقة قيمة اختبار (F) الذي يشير إلى صلاحية النموذج، و معنوية هذه النتائج عند مستوى دلالة أقل من

(0.05). و بالإضافة الي ذلك، أظهرت نتائج التحليل الإحصائي ان قيمة (B) تراوحت بين (0.511 – 0.640) و ان كل بعد (عند افتراض ثبات الابعاد الاخرى) تغيرا بمقدار وحدة واحدة فإن الاداء يتغير بنسبة (51.1% – 64%). وبناءً على النتائج السابقة فقد انتج اختبار هذه الفرضيات عن رفض الفرضيات العدمية، وقبول الفرضيات البديلة.

جدول رقم (4) نتائج اختبار الفرضيات الفرعية من الفرضية الرئيسية الثانية
(علاقات الارتباط ومعنوية الانحدار البسيط)

| المحور | معامل الارتباط R | معامل التحديد R-Square | قيمة F | الدلالة Sig | قيمة B | قيمة T | الدلالة Sig |
|-----------------------|------------------|------------------------|--------|-------------|--------|--------|-------------|
| العلاقة مع الموردين | 0.637 | 0.505 | 77.308 | 0.000 | 0.633 | 10.582 | 0.000 |
| العمليات الداخلية | 0.708 | 0.609 | 90.066 | 0.000 | 0.64 | 12.509 | 0.000 |
| العلاقة مع الوسطاء | 0.498 | 0.431 | 69.388 | 0.000 | 0.511 | 9.22 | 0.000 |
| العلاقة مع العملاء | 0.654 | 0.578 | 82.654 | 0.000 | 0.649 | 11.026 | 0.000 |
| المشاركة في المعلومات | 0.52 | 0.497 | 70.982 | 0.000 | 0.524 | 10.005 | 0.000 |

*دالة احصائيا عند مستوي (0.05).

4. الاستنتاجات

استناداً الى نتائج التحليل الإحصائي للبيانات لعينة الدراسة خرجت الدراسة بمجموعة من الاستنتاجات و النتائج التي مكنت من تقديم التوصيات ذات الأهمية المنطقية لمجتمع الدراسة وهي:

4.1 الاستنتاجات من نتائج الفرضية الرئيسية الاولى:

اظهرت نتيجة الدراسة ان هناك تطبيقاً لممارسات إدارة سلسلة التوريد بدرجة كبيرة بشركة النسيم للصناعات الغذائية حيث كانت علي النحو الآتي:

- العمليات الداخلية: اهتمام الشركة بهذا البعد يأتي في المركز الاول.
- العلاقة مع العملاء: اهتمام الشركة بهذا البعد يأتي في المركز الثاني.
- العلاقة مع الموردين: اهتمام الشركة بهذا البعد يأتي في المركز الثالث.
- المشاركة في المعلومات: اهتمام الشركة بهذا البعد يأتي في المركز الرابع.
- العلاقة مع الوسطاء: اهتمام الشركة بهذا البعد يأتي في المركز الخامس و الاخير.

4.2 الاستنتاجات من نتائج الفرضية الرئيسية الثانية:

يوجد دور للممارسات ادارة سلسلة التوريد في تحسين أداء شركة النسيم للصناعات الغذائية وهذا يزيد من أهمية الحرص على تطبيق هذه الممارسات في هذه الشركة؛ كونها تؤدي الى تحسين الاداء وهو الهدف المطلوب خصوصاً ان هذا الاداء مرتبط بأداء العمليات. حيث نلاحظ ان تحسين الأداء له تأثير فعال من خلال تقليل التكلفة و زيادة تحسين الجودة وكلاهما له اثر مالي في تقليل التكاليف، الخسائر مما يؤدي إلي زيادة الربحية و المرونة و سرعة التسليم اللذين لهما اثر كبير على رضا العملاء. و كنتيجة، كل هذا يؤدي الى زيادة المبيعات و الحصة السوقية اللتين تعتبران اهداف طويلة المدى للأداء كما يمكن إضافة بعض الاستنتاجات المستخلصة من خلال نتائج الفرضيات الفرعية للفرضية الرئيسية الثانية كالاتي:

- من خلال نتائج الدراسة، يتضح أن هناك عوامل مختلفة تلعب أدواراً متفاوتة في تحسين الأداء العام. حيث يحتل البعد المتعلق بالعمليات الداخلية المكانة الأولى من حيث تأثيره على تحسين الأداء، مما يشير إلى أن تحسين الكفاءة الداخلية وتنظيم العمليات يعد من العوامل الأساسية التي تساهم في زيادة فعالية الأداء بشكل كبير.
- في المرتبة الثانية، يأتي البعد المتعلق بالعلاقة مع العملاء وهو عنصر مهم في تحسين الأداء حيث يعكس أهمية العلاقة الوثيقة مع العملاء واحتياجاتهم في تحسين الخدمات أو المنتجات المقدمة، مما يساهم في بناء ولاء العملاء وزيادة رضاهم.
- أما البعد المتعلق بالعلاقة مع الموردين فيحتل المركز الثالث، مما يدل على أهمية التواصل والتعاون مع الموردين لضمان جودة المواد والخدمات وهو ما يؤثر إيجاباً على الأداء العام للمؤسسة.
- في المركز الرابع، نجد البعد المتعلق بمشاركة المعلومات والذي يظهر دوراً متوسطاً في تحسين الأداء. وهذا يشير إلى أن تبادل المعلومات بين مختلف الأطراف قد يساعد في تعزيز التعاون واتخاذ قرارات أفضل، ولكنه لا يعد العامل الأهم مقارنة بالعوامل الأخرى.
- وأخيراً، يظهر أن البعد المتعلق بالعلاقة مع الوسطاء له تأثير ضعيف على تحسين الأداء حيث يحتل المركز الأخير. مما يعكس أن دور الوسطاء في هذه الدراسة لا يعد ذو تأثير كبير مقارنة ببقية الأبعاد الأخرى في تحسين الأداء العام.

بناءً على كل هذه الاستنتاجات، يمكن القول أن التركيز على تحسين العمليات الداخلية وبناء علاقات قوية مع العملاء والموردين يعد من الأولويات التي يجب أن تركز عليها الشركات لتحقيق تحسين ملحوظ في أدائها.

5. التوصيات

إستناداً إلي النتائج المتحصل عليها، توصي الدراسة بتعزيز الاهتمام بتطبيق ممارسات إدارة سلسلة التوريد بالشركات لما لها من تأثير كبير في تحسين أداء العمليات من خلال تقليل التكاليف وتحسين الجودة مما يؤدي إلى زيادة الربحية. كما أن إدارة سلسلة التوريد تساهم في زيادة مرونة العمليات وسرعة التسليم مما يعزز رضا العملاء وبالتالي يؤدي إلى زيادة المبيعات

والحصة السوقية. بالإضافة الي ذلك، تبين ان هناك نقاط قوة غير مستغلة كما ان هناك ضعف ونقائص لم تستدرکها بعد وعليها تجاوزها لزيادة فعالية سلسلة التوريد وتعزيز تنافسيتها، كما يمكن تقديم مجموعة من النقاط على ضوء ما تم استخلاصه وذلك على النحو التالي:

1. التركيز على تحسين العلاقة مع الوسطاء والمشاركة في المعلومات: يجب الاهتمام بشكل أكبر بتطبيق بعد العلاقة مع الوسطاء وبعُد المشاركة في المعلومات، نظرًا لضعف تأثير هذين البعدين مقارنة بالأبعاد الأخرى. وبالتالي، سيكون من المفيد زيادة التركيز على تحسين هذه العلاقات لتعزيز الأداء العام.
2. يجب على الشركات تبني النهج الاستراتيجي في إدارة سلسلة التوريد الذي يركز على بناء علاقات طويلة الأمد مع الموردين بالإضافة إلى تعزيز التواصل الفعال والشراكة معهم. إن الكفاءة في إدارة سلسلة التوريد تمثل العنصر الأساسي لنجاح المنظمة على المدى الطويل. و لذلك ينبغي على الشركات العمل على توفير العناصر التي تدعم مرونة سلسلة التوريد لديها، خصوصاً في حال توفر عدد من الموردين المؤهلين لتلبية احتياجاتها من المواد، سواء في دفعات كبيرة أو طلبات منفصلة، مع القدرة على نقل هذه المواد باستخدام وسائل نقل متعددة. ومن الضروري أيضاً أن يكون هناك تنسيق محكم بين الشركة ومورديها خاصة في حالات زيادة الطلب من اجل تجنب تراكم المخزون والحفاظ على مستويات مخزون معتدلة.
3. تعزيز الاهتمام بالأبعاد الأكثر تأثيراً في الأداء: يجب إعطاء الأولوية لبعُد العمليات الداخلية، ثم بُعد العلاقة مع العملاء، وبعد ذلك لبعُد العلاقة مع الموردين. إن تعزيز هذه الأبعاد سيسهم بشكل كبير في تحسين الأداء ويجب أن يكون هناك متابعة مستمرة لتحسين هذه العوامل.
4. يُوصى بدمج إدارة سلسلة التوريد بشكل فعال في الهيكل التنظيمي للشركات، بحيث تُدار بشكل مستقل بدلاً من أن تكون مرتبطة بعدد من الإدارات المنفصلة مثل التخطيط، المشتريات، المخازن والتوزيع. اي أن إدارة سلسلة التوريد لا يجب أن تكون مقسمة أو موزعة على هذه الإدارات بشكل مستقل بل ينبغي أن تكون تحت إشراف إدارة موحدة ومنكاملة تعمل على تنسيق جميع الأنشطة المرتبطة بسلسلة التوريد من بداية عملية شراء المواد الخام وصولاً إلى تسليم المنتج النهائي للعميل. هذا التوجه يساهم في تحسين التنسيق والتعاون بين كافة الأنشطة المتعلقة بسلسلة التوريد.



Gharyan University Journal of Engineering Science (GUJES)

Website: <http://gujes.gu.edu.ly>

email: gujes@gu.edu.ly



قائمة المراجع:

- [1] Chopra, S., & Meindl, P. (2019). *Supply Chain Management: Strategy, Planning, and Operation*. Pearson.
- [2] Christopher, M. (2016). *Logistics & Supply Chain Management*. FT Publishing.
- [3] Mentzer, J. T., DeWitt, W., Keebler, J. S., Min, S., Nix, N. W., Smith, C. D., & Zacharia, Z. G. (2001). "Defining Supply Chain Management." *Journal of Business Logistics*, 22(2), 1-25.
- [4] Lambert, D. M., & Cooper, M. C. (2000). "Issues in Supply Chain Management." *Industrial Marketing Management*, 29(1), 65-83.
- [5] Stevens, G. C., & Johnson, M. (2016). "Integrating the Supply Chain... 25 Years On." *International Journal of Physical Distribution & Logistics Management*, 46(1), 19-42.
- [6] Ivanov, D. (2020). *Introduction to Supply Chain Resilience*. Springer.